Electronic supplementary information for:

Achieving ultra-narrow bandgap non-halogenated non-fullerene acceptor via vinylene π-bridges for efficient organic solar cells

Jiefeng Hai,‡[a b] Siwei Luo,‡[d] Han Yu,‡[d] Honggang Chen,[c] Zhenhuan Lu,[b] Ling Li,*[b] Yingping Zou,*[c] He Yan*[a, d]

[a] *HKUST-Shenzhen Research Institute No. 9 Yuexing 1st Road, Hi-tech Park, Nanshan Shenzhen 518057, China. E-mail: hyan@ust.hk*

[b] *Guangxi Key Laboratory of Electrochemical and Magneto-Chemical Functional Materials, Guilin University of Technology, Guilin 541004, Guangxi, China. E-mail: 6614034@glut.edu.cn*

[c] *College of Chemistry and Chemical Engineering, Central South University, Changsha 410083, Hunan, China. E-mail: yingpingzou@csu.edu.cn*

[d] *Department of Chemistry and Hong Kong Branch of Chinese National Engineering Research Center for Tissue Restoration & Reconstruction, Hong Kong University of Science and Technology (HKUST), Clear Water Bay, Kowloon, Hong Kong, China*

‡ *These authors contributed equally to this work.*

**Corresponding authors:*

hyan@ust.hk (H. Y.); 6614034@glut.edu.cn (L. L.); yingpingzou@csu.edu.cn (Y. Z.)

1. General Measurement and Characterization

^{1}H NMR and ^{13}C NMR spectra of intermediates and target small molecule were recorded on a Bruker ADANCE 400 and75 MHz NMR spectrometer using d-chloroform as solvent at room temperature. Chemical shift $CHCl_3$ (δ = 7.26 ppm for ^{1}H NMR and δ = 77.0 ppm for ^{13}C NMR). UV-Vis spectra were measured using a Shimadzu UV-2600 recording spectrophotometer. Cyclic voltammogram (CV) measurements of NFAs thin films were conducted on a CHI660E electrochemical workstation using glassy carbon as the working electrode, Pt wire as the counter electrode, and Ag/AgCl as the reference electrode in 0.1 mol L^{-1} tetrabutylammonium hexafluorophosphate (Bu_4NPF_6) acetonitrile solutions and at a scan rate of 20 mV s^{-1}.

2. Experimental procedures

Compound **1** and compound **2** were synthesized according to the previous reported methods.[1, 2] The bis(triphenylphosphine)palladium(II) dichloride [$Pd(PPh_3)_2Cl_2$], triphenylphosphine (PPh_3), N-methyl pyrrolidone (NMP), 5-(bromomethyl)undecane, bromide, 1,1-dicyanomethylene-3-indanone,phosphorus oxychloride, anhydrous 1,2-dichloroethane, tributyl(1,3-dioxolan-2-ylmethyl) phosphonium pyridine and reagents were purchased from J&K and Alfa Asia Chemical Co. Tetrahydrofuran (THF) was further dried by using sodium under 110℃ refluxing condition.

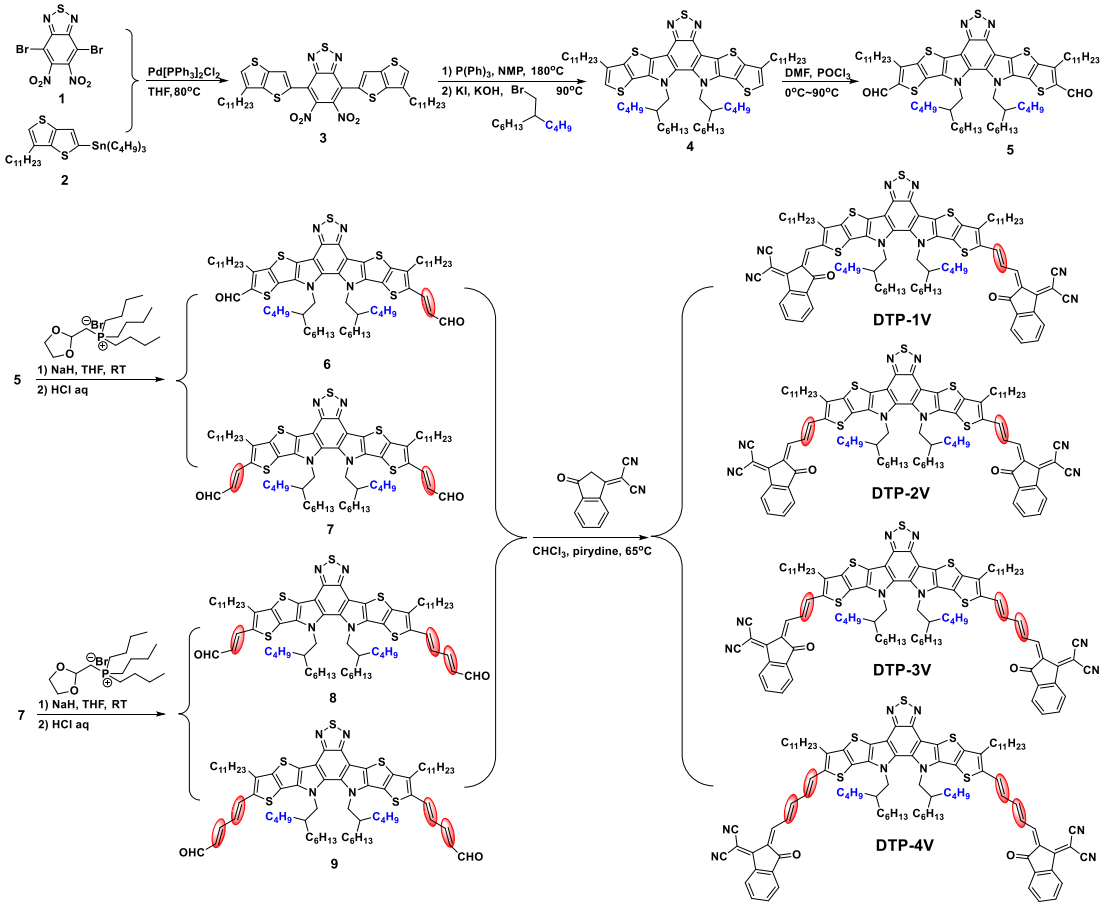

Scheme S1. Synthesis of four Y6 congeners.

Compound **4** was synthesized according to the literatures with some modification. Synthesized of compound **6** and **8** by Witting reaction, but the symmetric and unsymmetrical products were got at same time, where the yield of the unsymmetrical desired target small molecule was not high.

Synthesis of 5,6-dinitro-4,7-bis(6-undecylthieno[3,2-b]thiophen-2-yl)benzo[c] [1,2,5]thiadiazole (3)

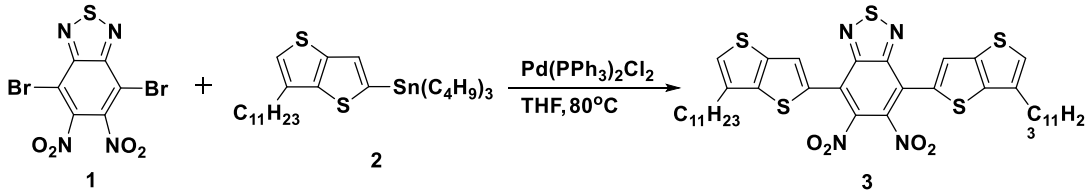

Compound **1** (4.0 g, 10 mmol), compound **2** (15.2 g, 26 mmol), and $Pd(PPh_3)_2Cl_2$ (366 mg, 0.52 mmol) were dissolved in anhydrous THF (60 mL) and stirred at 80°C for 6 h under nitrogen atmosphere. The reaction mixture was allowed to cool to room

temperature and then concentrated under vacuum. A red solid Compound **3** was obtained by recrystallization with petroleum ether (100 mL) (6.7 g, 79% yield). ^{1}H NMR (400 MHz, $CDCl_3$) δ 7.71 (s, 2H), 7.18 (s, 2H), 2.78 (t, *J* = 7.5 Hz, 4H), 1.78 (dd, *J* = 14.5, 7.3 Hz, 4H), 1.35-1.22 (m, 32H), 0.87 (t, *J* = 6.3 Hz, 6H).

Synthesis of 12,13-bis(2-butyloctyl)-3,9-diundecyl-12,13-dihydro-[1,2,5]thiadiazolo[3,4-e]thieno[2'',3'':4',5']thieno[2',3':4,5]pyrrolo[3,2-g]thieno[2',3':4,5]thieno[3,2-b]indole (4)

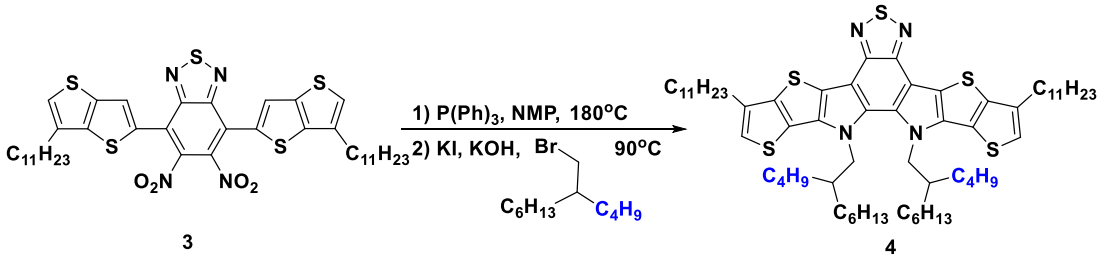

3 4

Compound **3** (2.5 g, 3 mmol) and PPh_3 (8.0 g, 30 mmol) were dissolved in the anhydrous N-methyl pyrrolidone (NMP, 40 mL) under nitrogen atmosphere. The mixture was stirred at 180°C for 24 h. After cooled to room temperature, 5-(bromomethyl)undecane (3.8 g, 15 mmol), potassium iodide (0.511 g, 3 mmol), potassium hydroxide (1.73 g, 31 mmol), and NMP (40 mL) were added. The mixture was stirred at 90°C for 24 h under nitrogen atmosphere. After cooled to room temperature, the mixture was then poured into water (300 mL). The organic solution was extracted with CH_2Cl_2. The combined organic layers were washed with water, brine and dried with anhydrous $MgSO_4$. The bright orange solid compound **4** was obtained by column chromatography on silica gel using petroleum ether/dichloromethane (9/1, v/v) as the eluent (1.3 g, 40% yield). ^{1}H NMR (400 MHz, $CDCl_3$) 7.01 (s, 2H), 4.59 (d, *J* = 7.7 Hz, 4H), 2.82 (t, *J* = 7.6 Hz, 4H), 2.15-1.96 (m, 2H), 1.90-1.81 (m, 4H), 1.42-1.25 (m, 40H), 0.97-0.84 (m, 24H), 0.77-0.50 (m, 18H). ^{13}C NMR (101 MHz, $CDCl_3$) δ 147.76, 142.18, 136.92, 131.80, 123.77, 122.88, 119.36, 111.59, 108.44, 55.07, 38.74, 36.22, 35.90, 32.00, 31.69 30.30, 29.60, 28.96, 28.14, 27.92, 25.42, 25.28, 23.03, 22.46, 14.36, 13.69.

Synthesis of 12,13-bis(2-butyloctyl)-3,9-diundecyl-12,13-dihydro-[1,2,5] thiadiazolo[3,4-e]thieno[2'',3'':4',5']thieno[2',3':4,5]pyrrolo[3,2-g]thieno[2',3':4,5]thieno[3,2-b]indole-2,10-dicarbaldehyde (5)

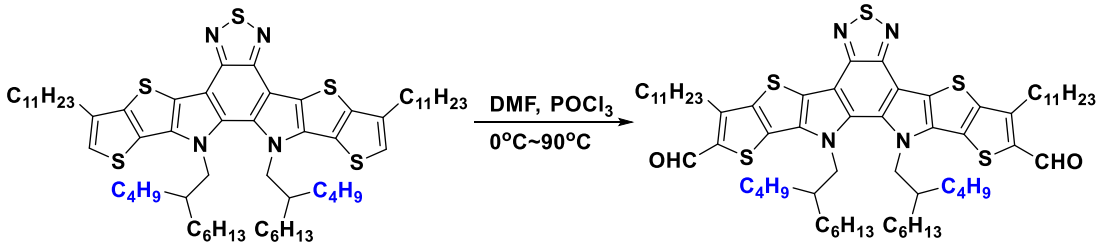

4 **5**

Phosphorus oxychloride (7.7 g, 50 mmol) was added dropwise slowly to anhydrous DMF (60 mL) at 0°C under nitrogen atmosphere and the mixture was then stirred for 2 h. A solution of compound **4** (1.8 g, 1.87 mmol) in anhydrous 1,2-dichloroethane (60 mL) was added dropwise to the mixture. After stirring at the same temperature for another 1.5 h, the mixture was heated to 90°C for 10 h. The reaction mixture was poured into water (150 mL) to quench the reaction, neutralized by NaOH and then extracted with CH_2Cl_2. The combined organic layers were washed with water and brine, dried over $MgSO_4$. Removing the solvent under reduced pressure and the crude product was purified with column chromatography on a silica gel using petroleum ether/dichloromethane (1/1, v/v) as the eluent to give a deep orange solid **5** (1.62 g, 85% yield). ^{1}H NMR (400 MHz, $CDCl_3$) δ 10.14 (s, 2H), 4.62 (d, *J* = 7.7 Hz, 4H), 3.20 (t, *J* = 7.6 Hz, 4H), 2.06-2.00 (m, 2H), 1.96-1.88 (m, 4H), 1.52-1.20 (m, 40H), 0.98-0.84 (m, 24H), 0.76-0.53 (m, 18H). ^{13}C NMR (101 MHz, $CDCl_3$) δ 181.82, 147.49, 146.89, 143.17, 137.03, 136.81, 132.97, 129.67, 127.40, 112.39, 55.23, 38.86, 31.91, 31.51, 30.50, 29.90, 29.84, 28.97, 28.17, 27.82, 25.20, 22.71, 22.43, 14.04, 13.70.

Synthesis of (E)-12,13-bis(2-butyloctyl)-10-(3-oxoprop-1-en-1-yl)-3,9-diundecyl -12,13-dihydro-[1,2,5]thiadiazolo[3,4-e]thieno[2'',3'':4',5']thieno[2',3':4,5]pyrrolo [3,2-g]thieno[2',3':4,5]thieno[3,2-b]indole-2-carbaldehyde (6)

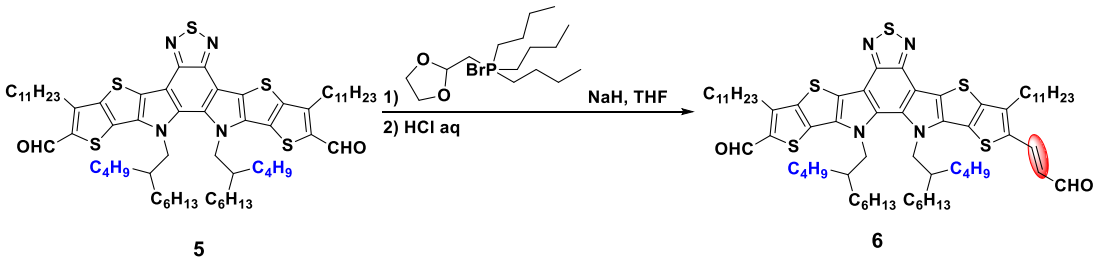

To a solution of the mixture of compound **5** (560 mg, 0.5 mmol) and tributyl(1,3-dioxolan-2-ylmethyl)phosphonium bromide (180 mg, 0.5 mmol) in anhydrous THF (30 mL) was added sodium hydride (60% wt%, 24 mg, 0.5 mmol) under nitrogen atmosphere, and the resulting solution was stirred at room temperature for 10 h. The reaction mixture was added HCl solution (10%, 10 mL) to quench the reaction and stirred at room temperature for 4-5 h. Then the mixture was extracted with CH_2Cl_2. The combined organic layers were washed with water and brine, dried over $MgSO_4$. Removing the solvent under reduced pressure and the crude product was purified with column chromatography on a silica gel using petroleum ether/dichloromethane (1/1, v/v) as the eluent to give a red solid **6** (108 mg, 34% yield). ^{1}H NMR (400 MHz, $CDCl_3$) δ 10.14 (s, 1H), 9.71 (d, *J* = 7.6 Hz, 1H), 7.78 (d, *J* = 15.3 Hz, 1H), 6.53 (dd, *J* = 15.8, 8.2 Hz, 1H), 4.61 (t, *J* = 7.7 Hz, 4H), 3.20 (t, *J* = 7.5 Hz, 2H), 2.99 (t, *J* = 7.5 Hz, 2H), 2.04 (s, 2H), 1.99-1.83 (m, 4H), 1.39-1.24 (m, 40H), 0.91-0.83 (m, 24H), 0.78-0.55 (m, 18H). ^{13}C NMR (101 MHz, $CDCl_3$) δ 192.45, 181.67, 147.42, 147.39, 146.80, 143.82, 143.26, 142.97, 142.62, 141.98, 137.01, 136.85, 136.56, 133.35, 133.13, 132.38, 129.65, 127.45, 125.80, 125.29, 125.06, 112.49, 111.99, 55.14, 38.91, 38.80, 38.68, 34.47, 34.06, 31.84, 31.47, 30.29, 30.11, 30.02, 29.95, 29.82, 29.62, 29.59, 29.57, 29.55, 29.45, 29.37, 29.32, 29.27, 28.29, 28.09, 28.00, 27.89, 27.83, 27.73, 27.66, 25.21, 25.13, 24.97, 24.93, 22.90, 22.62, 22.39, 22.37, 20.10, 19.10, 14.35, 14.10, 14.05, 13.89, 13.68, 13.65, 13.64, 13.62, 11.34. (MALDI-TOF) m/z calcd. for ($C_{94}H_{110}N_8O_2S_5$): 1164.6450. Found: 1164.6444.

Synthesis of (2E,2'E)-3,3'-(12,13-bis(2-butyloctyl)-3,9-diundecyl-12,13-dihydro-[1,2,5]thiadiazolo[3,4-e]thieno[2'',3'':4',5']thieno[2',3':4,5]pyrrolo[3,2-g]thieno[2',3':4,5]thieno[3,2-b]indole-2,10-diyl)diacrylaldehyde (7)

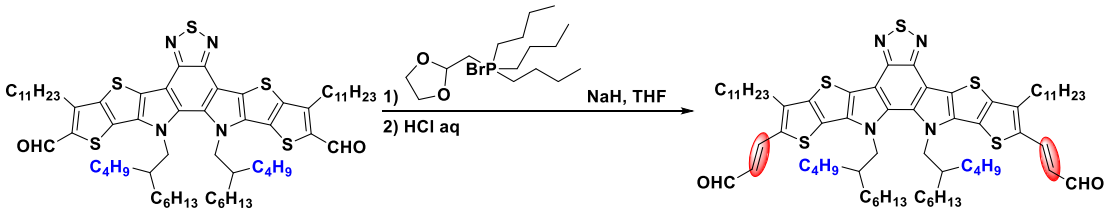

The synthesis of compound **7** was followed the same procedure of compound **6**. To a solution of the mixture of compound **5** (1.0 g, 0.87 mmol) and tributyl(1,3-dioxolan-2-ylmethyl)phosphonium bromide (713 mg, 1.93 mmol) in anhydrous THF (50 mL) was added sodium hydride (60% wt%, 105 mg, 2.63 mmol) under nitrogen atmosphere, and the resulting solution was stirred at room temperature for 10 h. The reaction mixture was added HCl solution (10%, 10 mL) to quench the reaction and stirred at room temperature for 4-5 h. Then the mixture was extracted with CH_2Cl_2. The combined organic layers were washed with water and brine, dried over $MgSO_4$. Removing the solvent under reduced pressure and the crude product was purified with column chromatography on a silica gel using petroleum ether/dichloromethane (1/1, v/v) as the eluent to give a bright red solid compound **7** (930 mg, 89% yield). ^{1}H NMR (400 MHz, $CDCl_3$) δ 9.70 (d, *J* = 7.6 Hz, 2H), 7.78 (d, *J* = 15.3 Hz, 2H), 6.52 (dd, *J* = 15.2, 7.6 Hz, 2H), 4.59 (d, *J* = 7.6 Hz, 4H), 2.99 (t, *J* = 7.5 Hz, 4H), 2.06-1.99 (m, 2H), 1.89-1.81 (m, 4H), 1.52-1.21 (m, 40H), 0.99-0.83 (m, 24H), 0.63 (m, 18H). ^{13}C NMR (101 MHz, $CDCl_3$) δ 192.72, 147.59, 143.86, 142.89, 142.23, 137.00, 133.41, 132.82, 126.12, 125.35, 125.32, 112.31, 55.25, 38.97, 32.04, 31.69, 30.45, 30.32, 30.17, 30.01,28.83, 29.79, 29.74, 29.68, 29.57, 29.46, 28.49, 27.88, , 25.37, 25.13, 22.82, 22.59, 14.26, 14.09, 13.88, 13.84. (MALDI-TOF) m/z calcd. for ($C_{94}H_{110}N_8O_2S_5$): 1190.6606. Found: 1190.6597.

Synthesis of (2E,4E)-5-(12,13-bis(2-butyloctyl)-10-((E)-3-oxoprop-1-en-1-yl)-3,9-diundecyl-12,13-dihydro-[1,2,5]thiadiazolo[3,4-e]thieno[2'',3'':4',5']thieno[2',3':4,5]pyrrolo[3,2-g]thieno[2',3':4,5]thieno[3,2-b]indol-2-yl)penta-2,4-dienal (8)

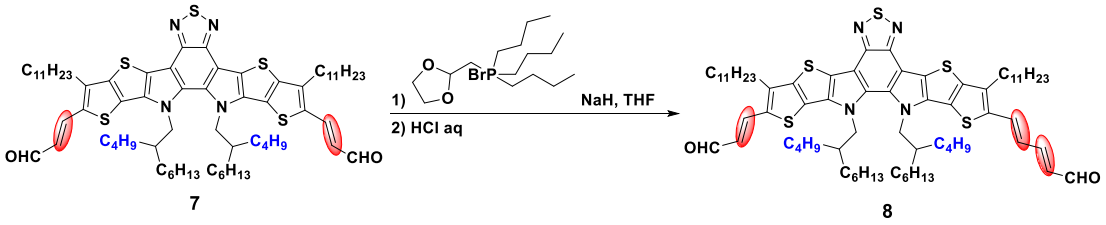

The synthesis of compound **8** was followed the same procedure of compound **6**. To a solution of the mixture of compound **7** (400 mg, 0.34 mmol) and tributyl(1,3-dioxolan-2-ylmethyl)phosphonium bromide (120 mg, 0.34 mmol) in anhydrous THF (30 mL) was added sodium hydride (60% wt%, 14 mg, 0.34 mmol) under nitrogen atmosphere, and the resulting solution was stirred at room temperature for 10 h. The reaction mixture was added HCl solution (10%, 10 mL) to quench the reaction and stirred at room temperature for 4-5 h. Then the mixture was extracted with CH_2Cl_2. The combined organic layers were washed with water and brine, dried over $MgSO_4$. Removing the solvent under reduced pressure and the crude product was purified with column chromatography on a silica gel using petroleum ether/dichloromethane (1/1, v/v) as the eluent to give a deep red solid compound **8** (150 mg, 37% yield). ^{1}H NMR (400 MHz, $CDCl_3$) δ 9.70 (d, *J* = 7.6 Hz, 1H), 9.63 (d, *J* = 7.9 Hz, 1H), 7.78 (d, *J* = 15.3 Hz, 1H), 7.32 (dt, *J* = 15.0, 5.5 Hz, 2H), 6.80 (dd, *J* = 14.7, 11.1 Hz, 1H), 6.52 (dd, *J* = 15.3, 7.6 Hz, 1H), 6.27 (dd, *J* = 15.0, 7.9 Hz, 1H), 4.59 (d, *J* = 7.2 Hz, 4H), 2.99 (t, *J* = 7.7 Hz, 2H), 2.92 (t, *J* = 7.6 Hz, 2H), 2.04 (s, 2H), 1.83 (dd, *J* = 13.6, 7.3 Hz, 4H), 1.50-1.21 (m, 34H), 1.13-0.84 (m, 30H), 0.82-0.48 (m, 18H). (MALDI-TOF) m/z calcd. for ($C_{94}H_{110}N_8O_2S_5$): 1216.6763. Found: 1216.6759.

Synthesis of (2E,2'E,4E,4'E)-5,5'-(12,13-bis(2-butyloctyl)-3,9-diundecyl-12,13-dihydro-[1,2,5]thiadiazolo[3,4-e]thieno[2'',3'':4',5']thieno[2',3':4,5]pyrrolo[3,2-g]thieno[2',3':4,5]thieno[3,2-b]indole-2,10-diyl)bis(penta-2,4-dienal) (9)

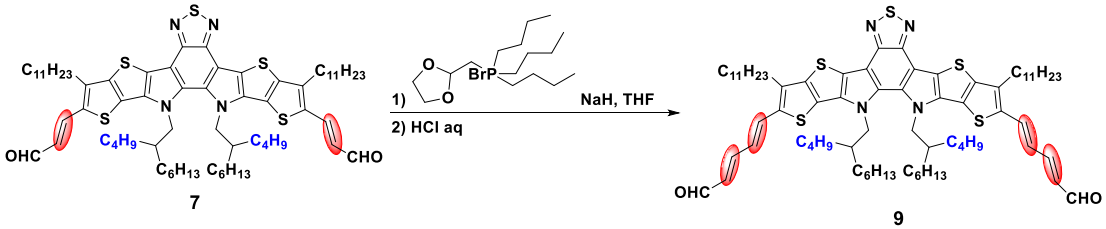

The synthesis of compound **9** was followed the same procedure of compound **6**. To a

solution of the mixture of compound **7** (134 mg, 0.11 mmol) and tributyl(1,3-dioxolan-2-ylmethyl)phosphonium bromide (91 mg, 0.25 mmol) in anhydrous THF (30 mL) was added sodium hydride (60% wt%, 13 mg, 0.33 mmol) under nitrogen atmosphere, and the resulting solution was stirred at room temperature for 10 h. The reaction mixture was added HCl solution (10%, 10 mL) to quench the reaction and stirred at room temperature for 4-5 h. Then the mixture was extracted with CH_2Cl_2. The combined organic layers were washed with water and brine, dried over $MgSO_4$. Removing the solvent under reduced pressure and the crude product was purified with column chromatography on a silica gel using petroleum ether/dichloromethane (1/1, v/v) as the eluent to give a deep red solid compound **9** (130 mg, 92% yield). ^{1}H NMR (400 MHz, $CDCl_3$) δ 9.63 (d, *J* = 7.9 Hz, 2H), 7.36-7.28 (m, 4H), 6.80 (dd, *J* = 14.8, 11.2 Hz, 2H), 6.27 (dd, *J* = 14.9, 7.8 Hz, 2H), 4.58 (d, *J* = 7.6 Hz, 4H), 2.92 (t, *J* = 7.6 Hz, 4H), 2.06 (s, 2H), 1.86-1.79 (m, 4H), 1.45-1.25 (m, 34H), 1.06-0.83 (m, 30H), 0.80-0.50 (m, 18H). (MALDI-TOF) m/z calcd. for ($C_{94}H_{110}N_8O_2S_5$): 1242.6919. Found: 1242.6904.

Synthesis of 2-((Z)-2-((E)-3-(12,13-bis(2-butyloctyl)-10-(((Z)-1-(dicyanomethylene)-3-oxo-1,3-dihydro-2H-inden-2-ylidene)methyl)-3,9-diundecyl-12,13-dihydro-[1,2,5]thiadiazolo[3,4-e]thieno[2'',3'':4',5']thieno[2',3':4,5]pyrrolo[3,2-g]thieno[2',3':4,5]thieno[3,2-b]indol-2-yl)allylidene)-3-oxo-2,3-dihydro-1H-inden-1-ylidene)malononitrile (BTP-1V)

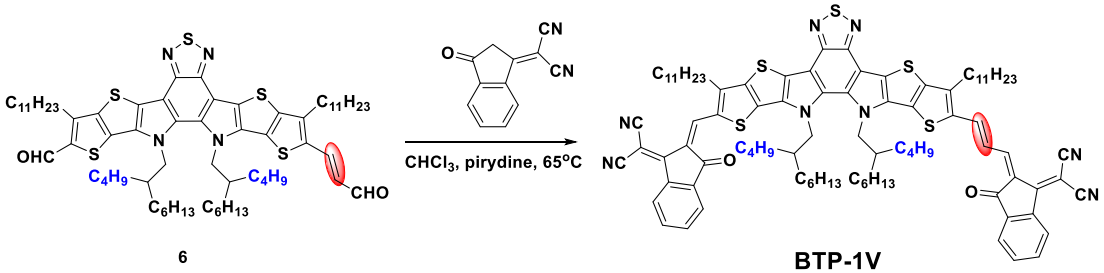

6 BTP-1V

Compound **6** (100 mg, 0.09 mmol) and 1,1-dicyanomethylene-3-indanone (67 mg, 0.32 mmol) were dissolved in chloroform (30 mL). Then pyridine (1.0 mL) was slowly added dropwise under nitrogen atmosphere. The mixture was stirred at 65°C overnight. After cooling to room temperature, the mixture was poured into methanol

(200 mL) and filtered. The residue was purified with column chromatography on silica gel using petroleum ether/dichloromethane (1/2, v/v) as the eluent to give a dark blue solid **BTP-1V** (110 mg, 85% yield). ^{1}H NMR (400 MHz, $CDCl_3$) δ 9.18 (s, 1H), 8.77-8.67 (m, 3H), 8.52 (d, *J* = 11.6 Hz, 1H), 7.94 (dd, *J* = 10.2, 5.0 Hz, 2H), 7.81-7.73 (m, 4H), 7.70 (d, *J* = 14.4 Hz, 1H), 4.75 (s, 2H), 4.66 (d, *J* = 7.3 Hz, 2H), 3.24 (t, *J* = 7.7 Hz, 2H), 3.02 (t, *J* = 7.6 Hz, 2H), 2.13 (s, 2H), 1.87 (dd, *J* = 15.0, 7.3 Hz, 4H), 1.53-1.24 (m, 30H), 1.20-0.84 (m, 34H), 0.84-0.55 (m, 18H). (MALDI-TOF) m/z calcd. for ($C_{92}H_{108}N_8O_2S_5$): 1517.7232. Found: 1517.7226.

Synthesis of (12,13-bis(2-butyloctyl)-3,9-diundecyl-12,13-dihydro-[1,2,5]thiadiazolo[3,4-e]thieno[2'',3'':4',5']thieno[2',3':4,5]pyrrolo[3,2-g]thieno[2',3':4,5]thieno[3,2-b]indole-2,10-diyl)bis(prop-2-en-3-yl-1-ylidene))bis(3-oxo-2,3-dihydro-1H-indene-2,1-diylidene))dimalononitrile (BTP-2V)

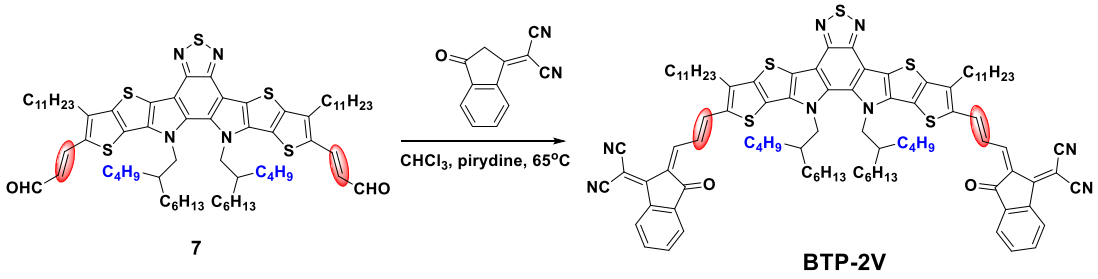

7 BTP-2V

The synthesis of **BTP-2V** was followed the same procedure of **BTP-1V**. Compound **7** (150 mg, 0.13 mmol) and 1,1-dicyanomethylene-3-indanone (98 mg, 0.50 mmol) were dissolved in chloroform (30 mL). Then pyridine (1.0 mL) was slowly added dropwise under nitrogen atmosphere. The mixture was stirred at 65°C overnight. After cooling to room temperature, the mixture was poured into methanol (200 mL) and filtered. The residue was purified with column chromatography on silica gel using petroleum ether/dichloromethane (1/2, v/v) as the eluent to give a dark blue solid **BTP-2V** (150 mg, 80% yield). ^{1}H NMR (400 MHz, $CDCl_3$) δ 8.71 (t, *J* = 11.3 Hz, 4H), 8.52 (d, *J* = 11.6 Hz, 2H), 7.92 (dd, *J* = 5.9, 2.2 Hz, 2H), 7.80-7.67 (m, 6H), 4.65 (d, *J* = 6.6 Hz, 4H), 3.02 (t, *J* = 7.5 Hz, 4H), 2.12 (s, 2H), 1.93-1.81 (m, 4H), 1.52-1.22 (m, 36H), 1.07-0.84 (m, 28H), 0.83-0.56 (m, 18H). (MALDI-TOF) m/z calcd. for ($C_{94}H_{110}N_8O_2S_5$): 1543.7389. Found: 1543.7380.

Synthesis of 3-(12,13-bis(2-butyloctyl)-1-(dicyanomethylene)-3-oxo-1,3-dihydro-2H-inden-2-ylidene)penta-1,3-dien-1-yl)-3,9-diundecyl-12,13-dihydro-[1,2,5]thiadiazolo[3,4-e]thieno[2'',3'':4',5']thieno[2',3':4,5]pyrrolo[3,2-g]thieno[2',3':4,5]thieno[3,2-b]indol-2-yl)allylidene)-3-oxo-2,3-dihydro-1H-inden-1-ylidene)malononitrile (BTP-3V)

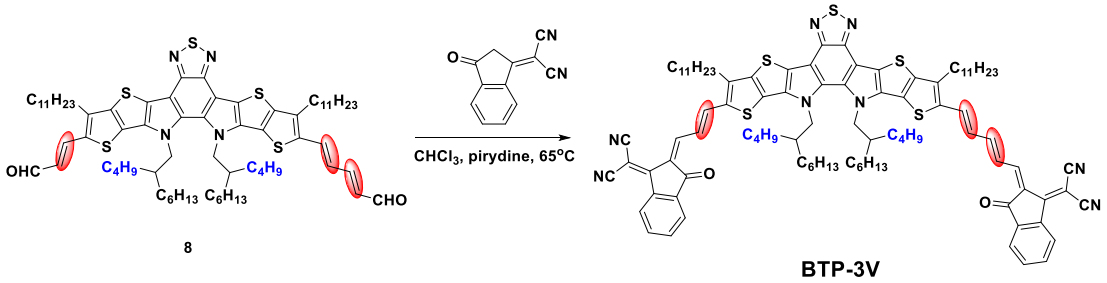

8 BTP-3V

The synthesis of **BTP-3V** was followed the same procedure of **BTP-1V**. Compound **13** (80 mg, 0.06 mmol) and 1,1-dicyanomethylene-3-indanone (51 mg, 0.26 mmol) were dissolved in chloroform (20 mL). Then pyridine (1.0 mL) was slowly added dropwise under nitrogen atmosphere. The mixture was stirred at 65°C overnight. After cooling to room temperature, the mixture was poured into methanol (200 mL) and filtered. The residue was purified with column chromatography on silica gel using petroleum ether/dichloromethane (1/2, v/v) as the eluent to give a dark blue solid **BTP-3V-IC** (83 mg, 80% yield). ^{1}H NMR (400 MHz, $CDCl_3$) δ 8.68 (t, *J* = 6.3 Hz, 3H), 8.52 (d, *J* = 11.7 Hz, 1H), 8.44 (d, *J* = 11.6 Hz, 1H), 8.32 (s, 1H), 7.91 (dd, *J* = 5.7, 1.7 Hz, 2H), 7.79-7.67 (m, 5H), 7.45-7.28 (m, 2H), 7.00 (s, 1H), 4.64 (d, *J* = 6.7 Hz, 4H), 3.01 (t, *J* = 7.3 Hz, 2H), 2.93 (t, *J* = 7.4 Hz, 2H), 2.11 (s, 1H), 1.90-1.78 (m, 4H), 1.49-1.23 (m, 34H), 1.10-0.84 (m, 30H), 0.83-0.48 (m, 18H). (MALDI-TOF) m/z calcd. for ($C_{96}H_{112}N_8O_2S_5$): 1569.7545. Found: 1569.7528.

Synthesis of (12,13-bis(2-butyloctyl)-3,9-diundecyl-12,13-dihydro-[1,2,5]thiadiazolo[3,4-e]thieno[2'',3'':4',5']thieno[2',3':4,5]pyrrolo[3,2-g]thieno[2',3':4,5]thieno[3,2-b]indole-2,10-diyl)bis(penta-2,4-dien-5-yl-1-ylidene))bis(3-oxo-2,3-dihydro-1H-indene-2,1-diylidene))dimalononitrile (BTP-4V)

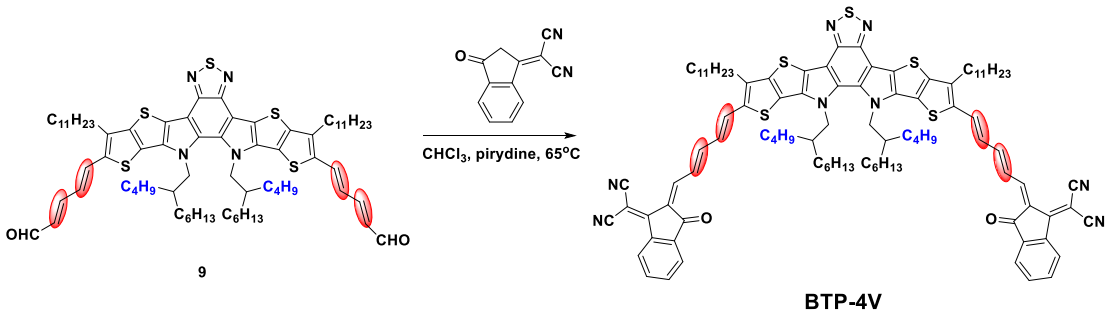

The synthesis of **BTP-4V** was followed the same procedure of **BTP-1V**. Compound **9** (130 mg, 0.1 mmol) and 1,1-dicyanomethylene-3-indanone (81 mg, 0.4 mmol) were dissolved in chloroform (40 mL). Then pyridine (1.0 mL) was slowly added dropwise under nitrogen atmosphere. The mixture was stirred at 65°C overnight. After cooling to room temperature, the mixture was poured into methanol (300 mL) and filtered. The residue was purified with column chromatography on silica gel using petroleum ether/dichloromethane (1/2, v/v) as the eluent to give a dark blue solid **BTP-4V** (135 mg, 82% yield). ^{1}H NMR (400 MHz, $CDCl_3$) δ 8.66 (d, *J* = 7.2 Hz, 2H), 8.43 (d, *J* = 11.8 Hz, 2H), 8.30 (s, 2H), 7.90 (d, *J* = 6.3 Hz, 2H), 7.78-7.69 (m, 4H), 7.46-7.28 (m, 4H), 6.97 (s, 2H), 4.64 (d, *J* = 7.3 Hz, 4H), 2.93 (t, *J* = 7.3 Hz, 4H), 2.11 (s, 2H), 1.88-1.77 (m, 4H), 1.50-1.22 (m, 34H), 1.09-0.85 (m, 30H), 0.83-0.54 (m, 18H). (MALDI-TOF) m/z calcd. for ($C_{98}H_{114}N_8O_2S_5$): 1595.7702. Found: 1595.7693.

3. ^{1}H and ^{13}C NMR spectra

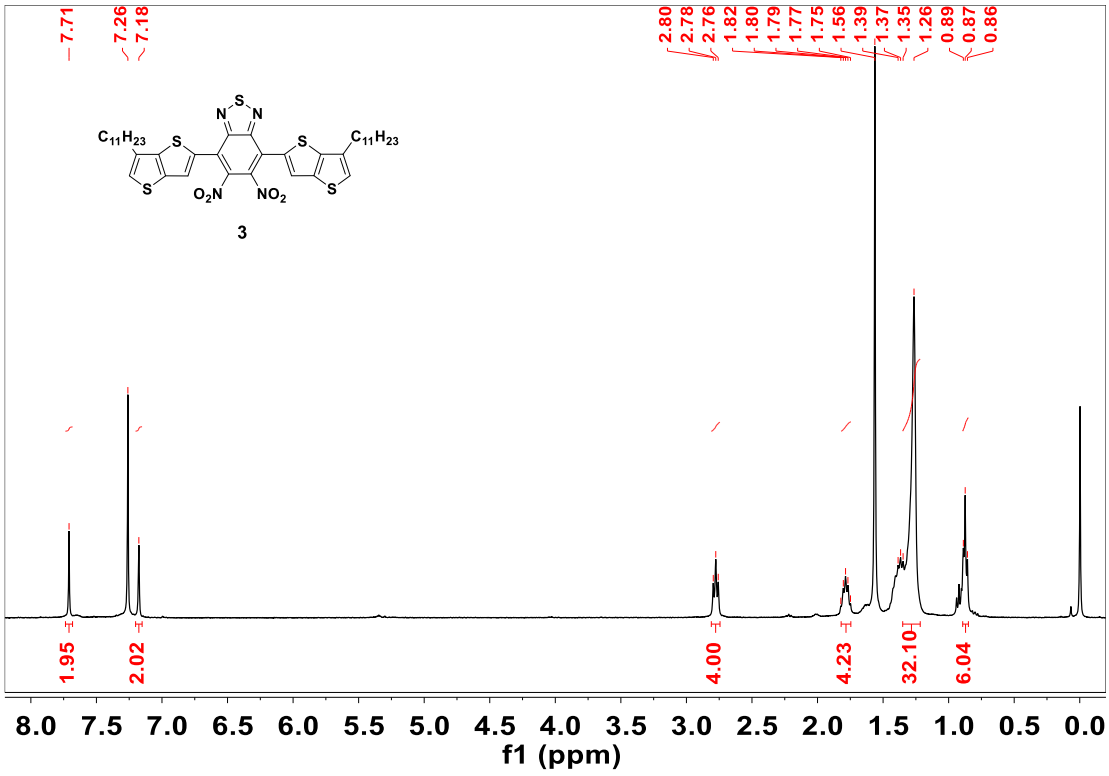

Fig. S1. ^{1}H NMR spectrum of compound 3 in $CDCl_3$

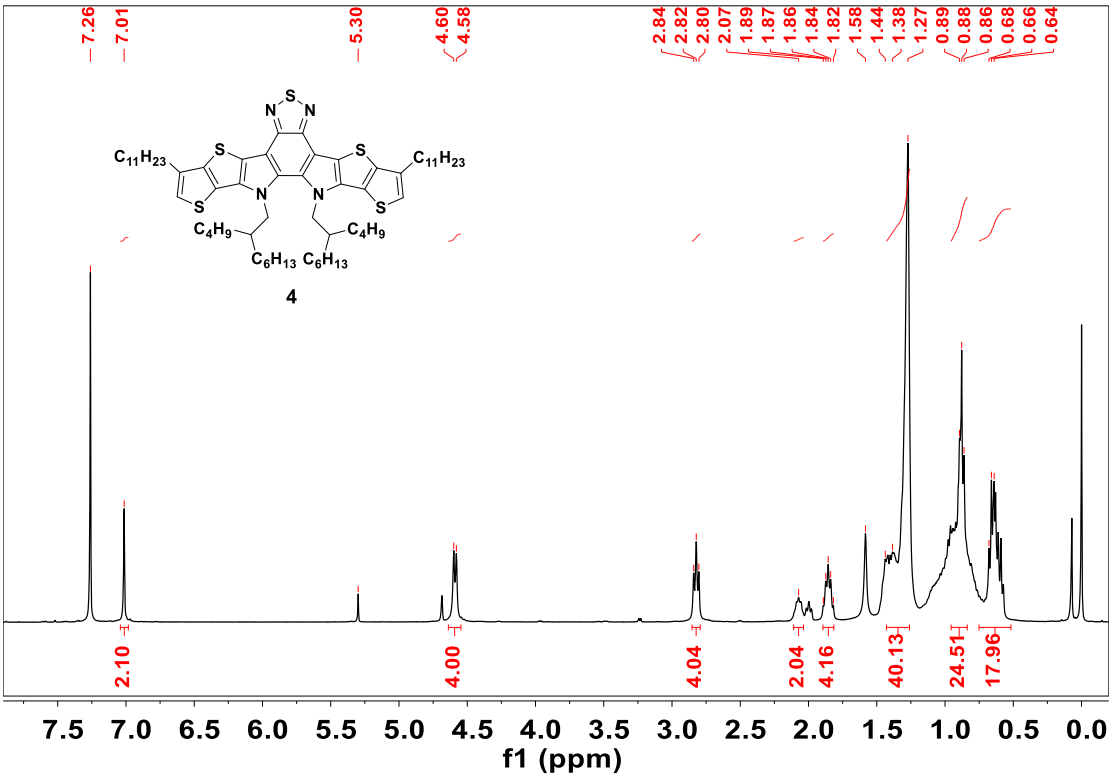

Fig. S2. ^{1}H NMR spectrum of compound 4 in $CDCl_3$

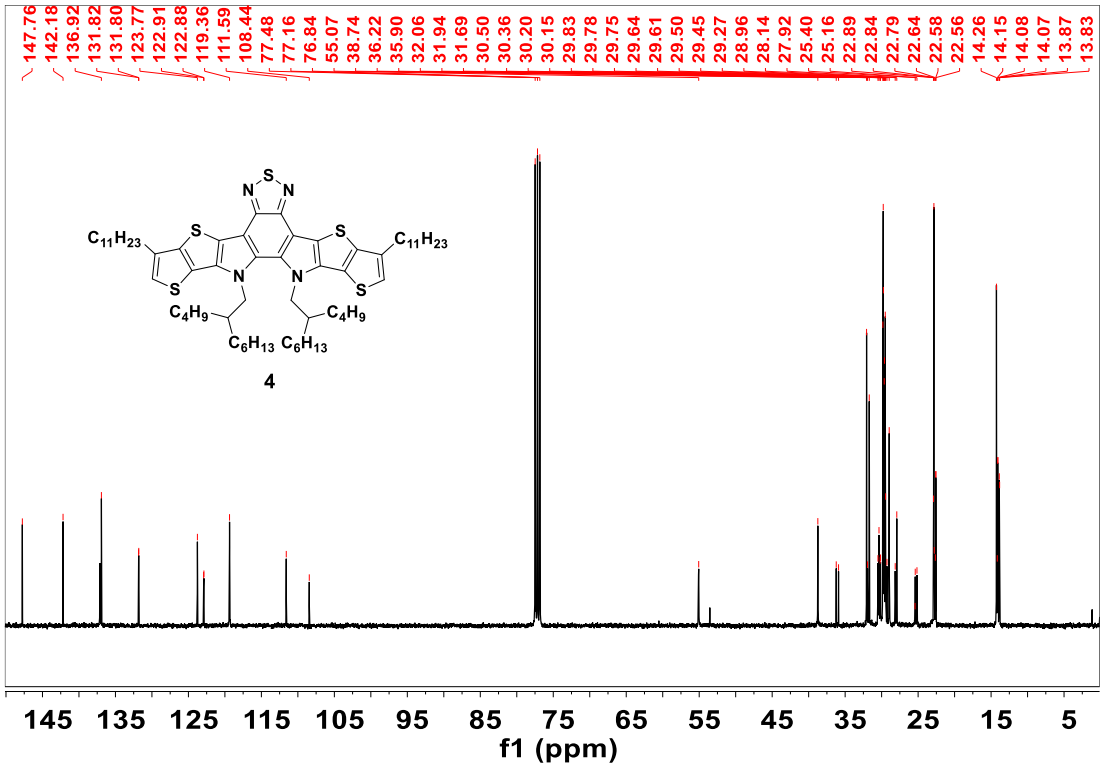

Fig. S3. ^{13}C NMR spectrum of compound 4 in $CDCl_3$

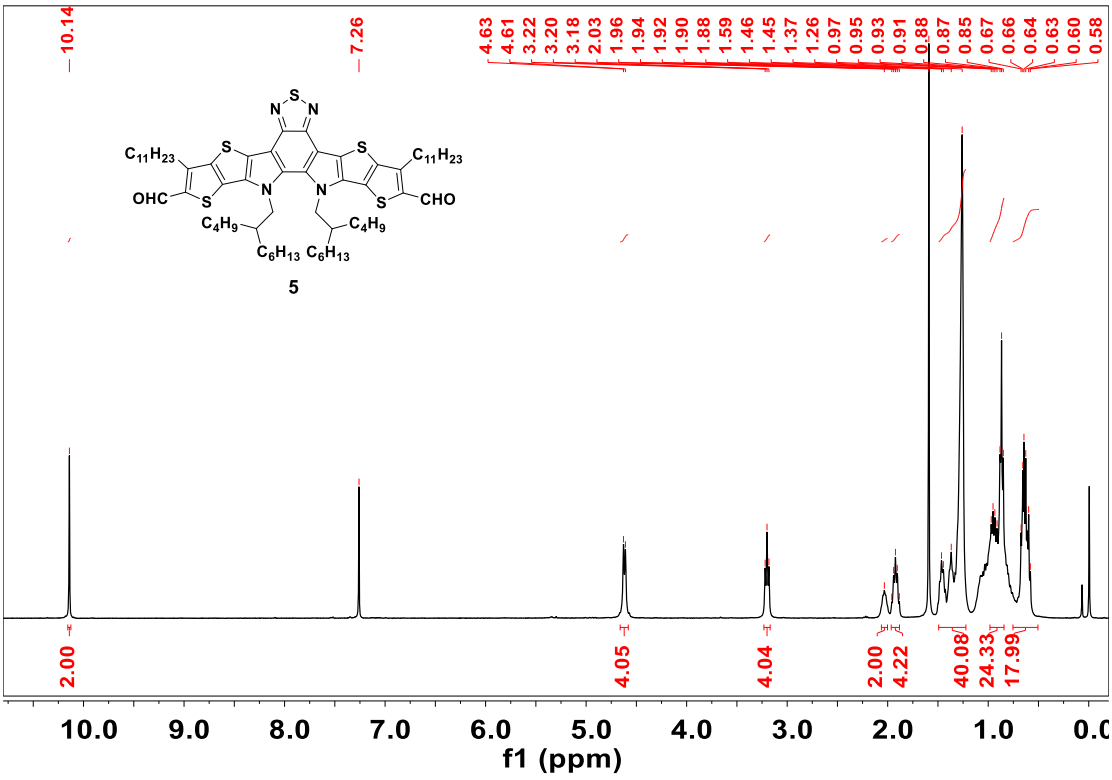

Fig. S4. ^{1}H NMR spectrum of compound 5 in $CDCl_3$

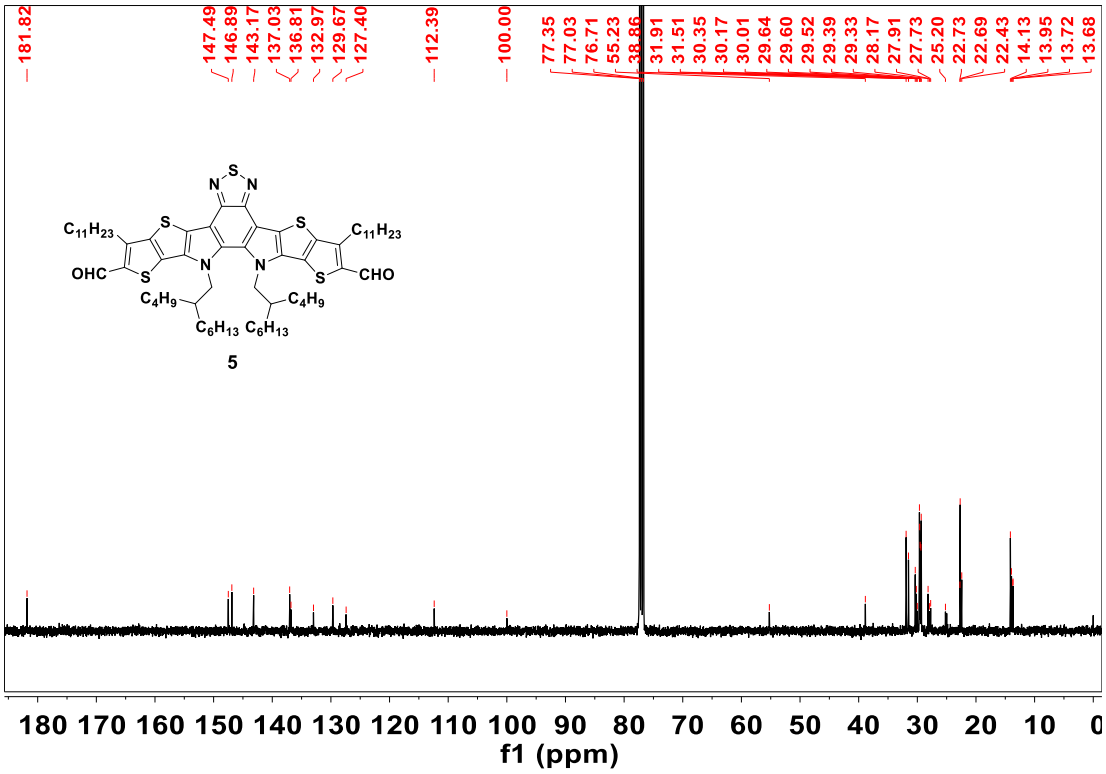

Fig. S5. ^{13}C NMR spectrum of compound 5 in $CDCl_3$

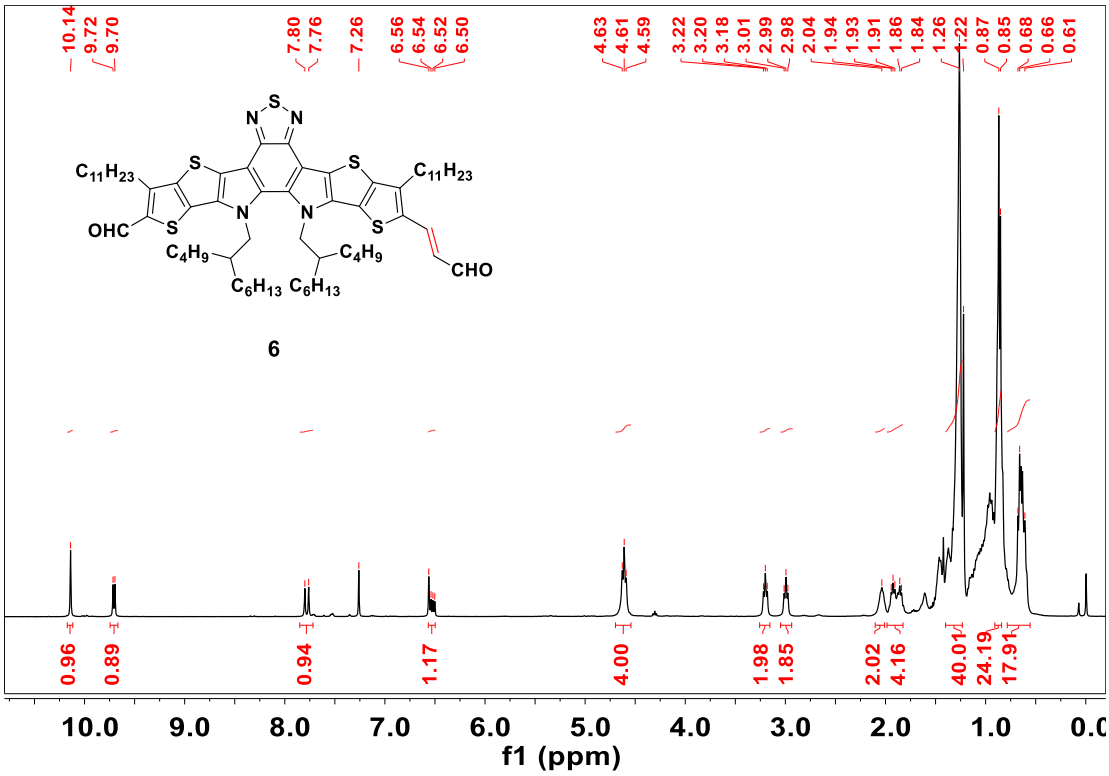

Fig. S6. ^{1}H NMR spectrum of compound 6 in $CDCl_3$

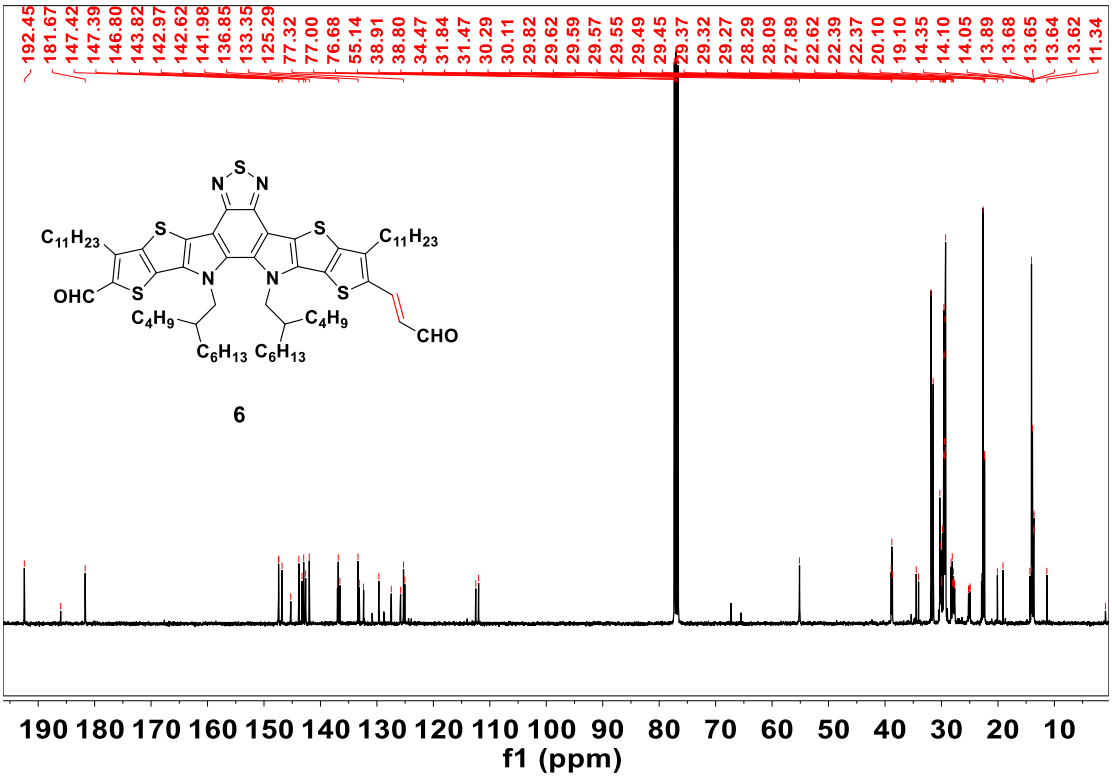

Fig. S7. ^{13}C NMR spectrum of compound 6 in $CDCl_3$

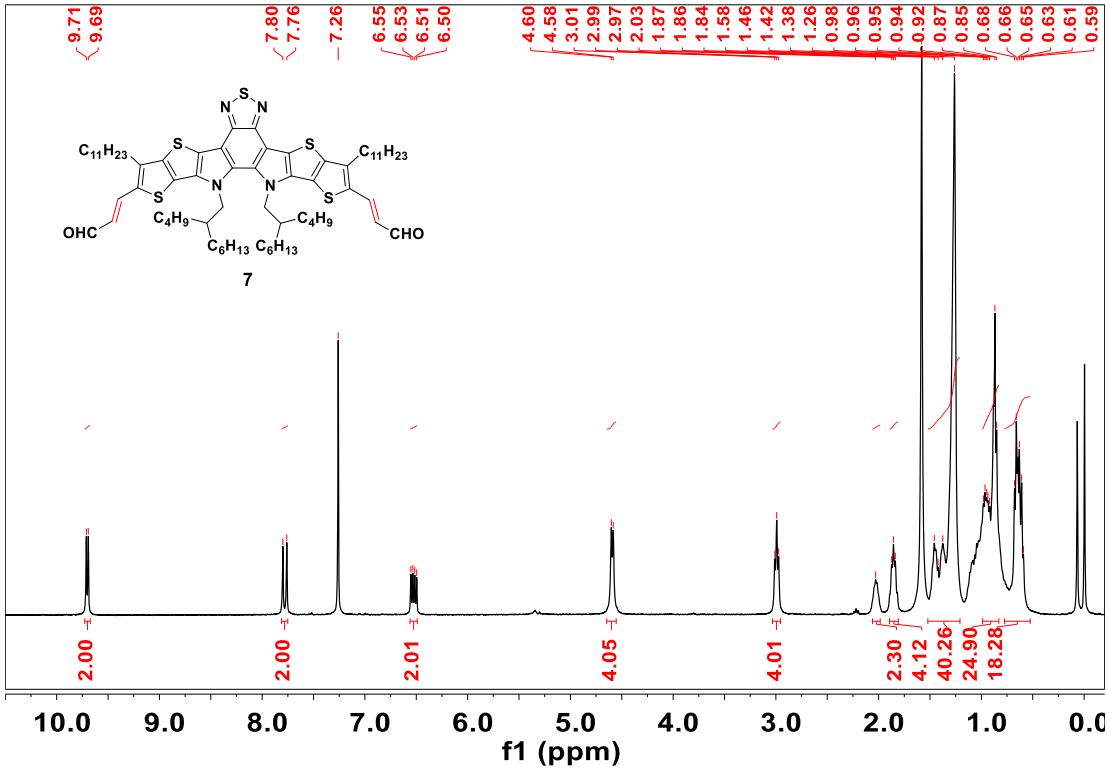

Fig. S8. ^{1}H NMR spectrum of compound 7 in $CDCl_3$

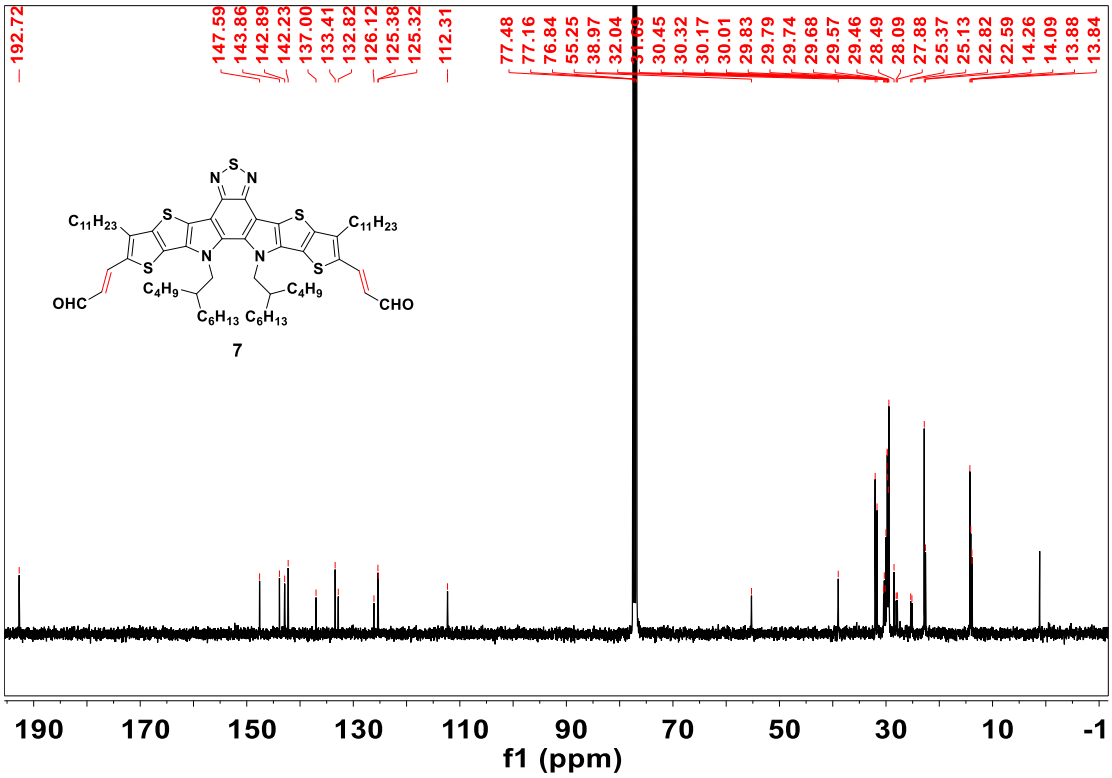

Fig. S9. ^{13}C NMR spectrum of compound 7 in $CDCl_3$

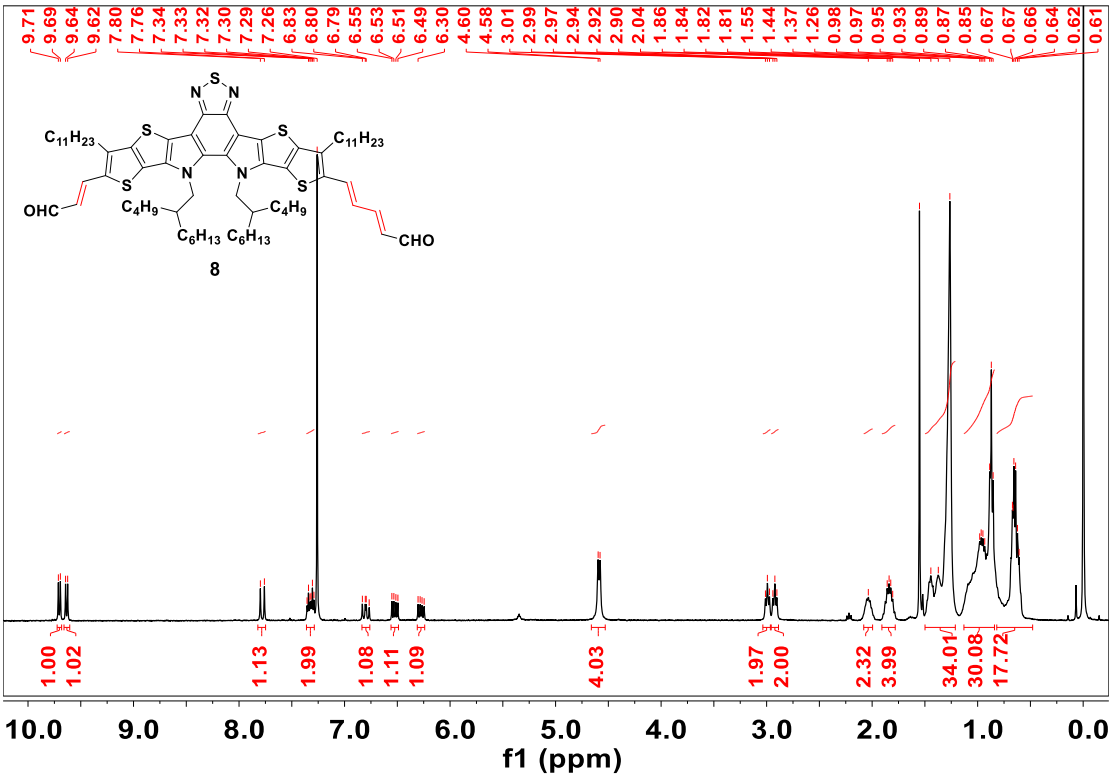

Fig. S10. ^{1}H NMR spectrum of compound 8 in $CDCl_3$

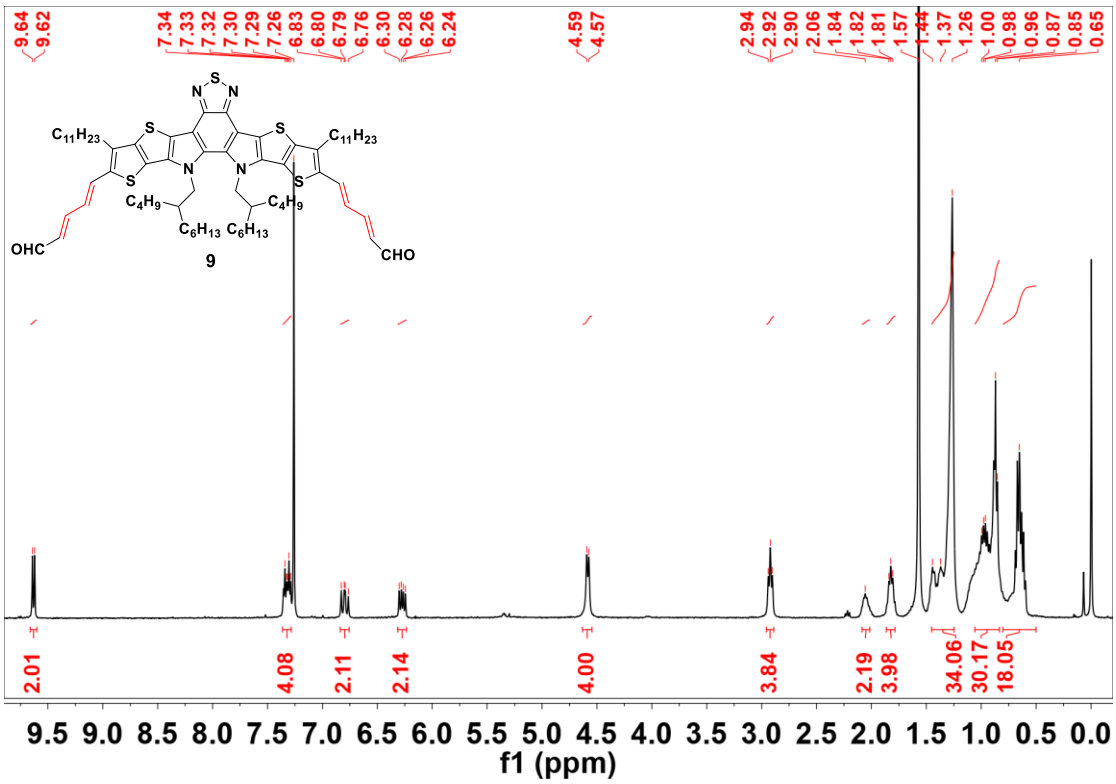

Fig. S11. ^{1}H NMR spectrum of 9 in $CDCl_3$

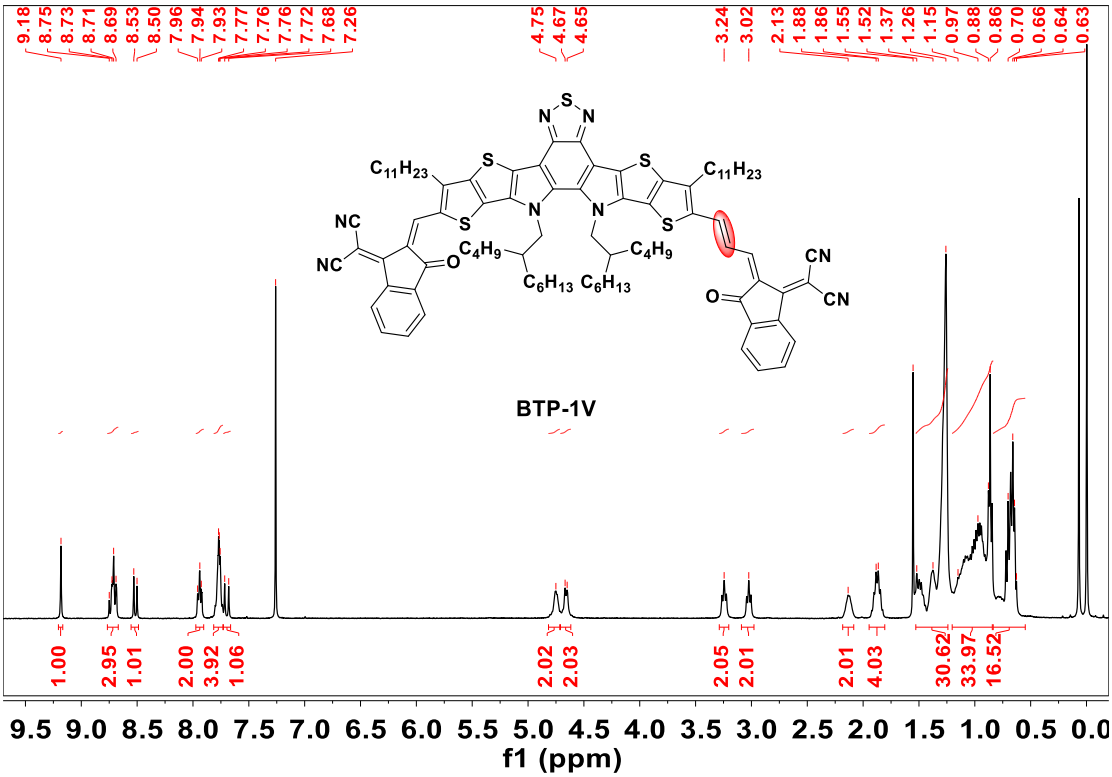

Fig. S12. ^{1}H NMR spectrum of compound BTP-1V in $CDCl_3$

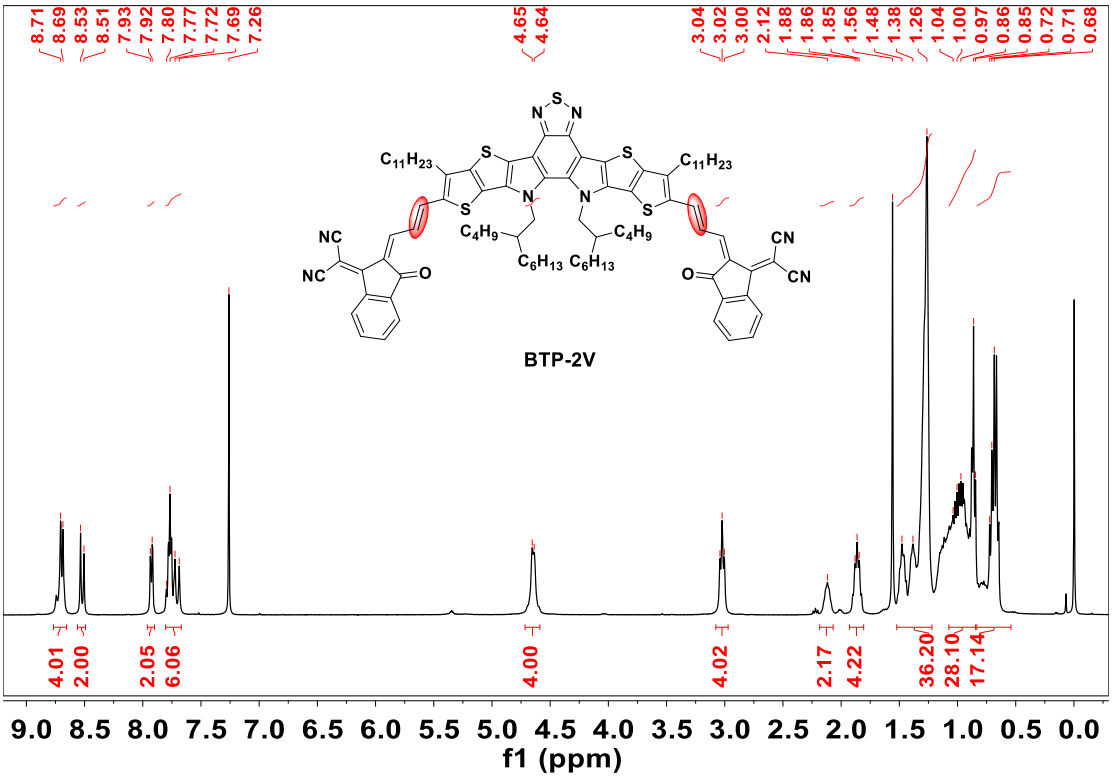

Fig. S13 ^{1}H NMR spectrum of compound BTP-2V in $CDCl_3$

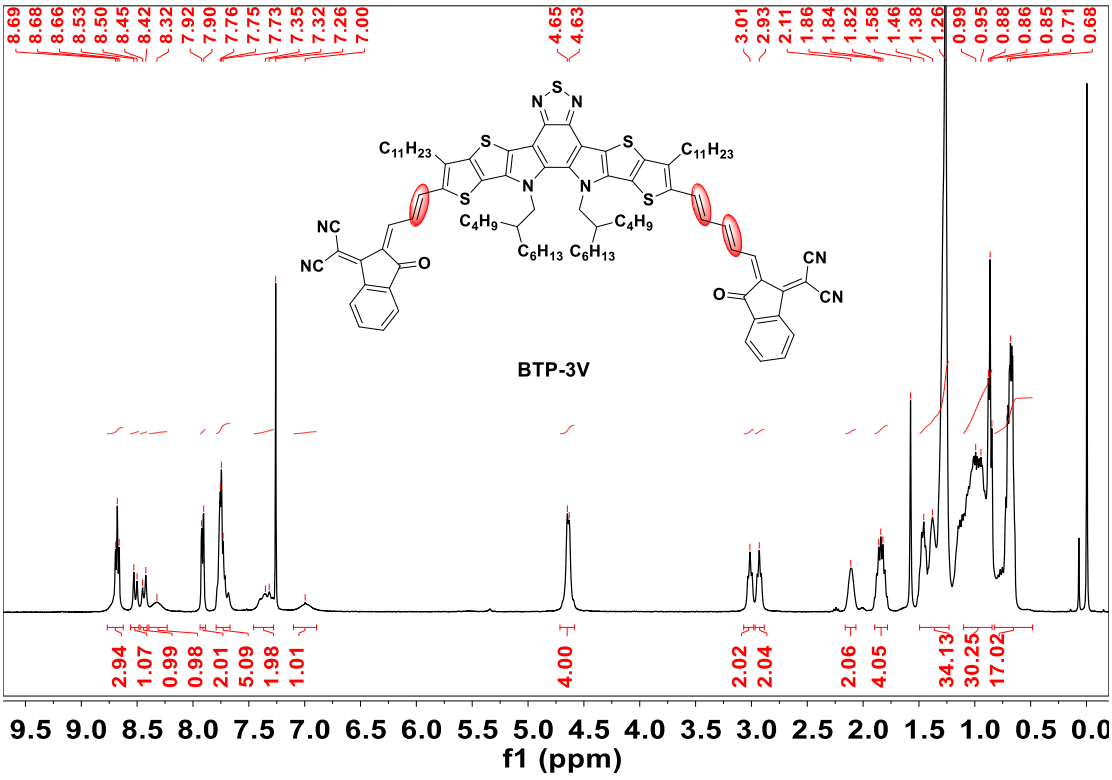

Fig. S14. ^{1}H NMR spectrum of BTP-3V in $CDCl_3$

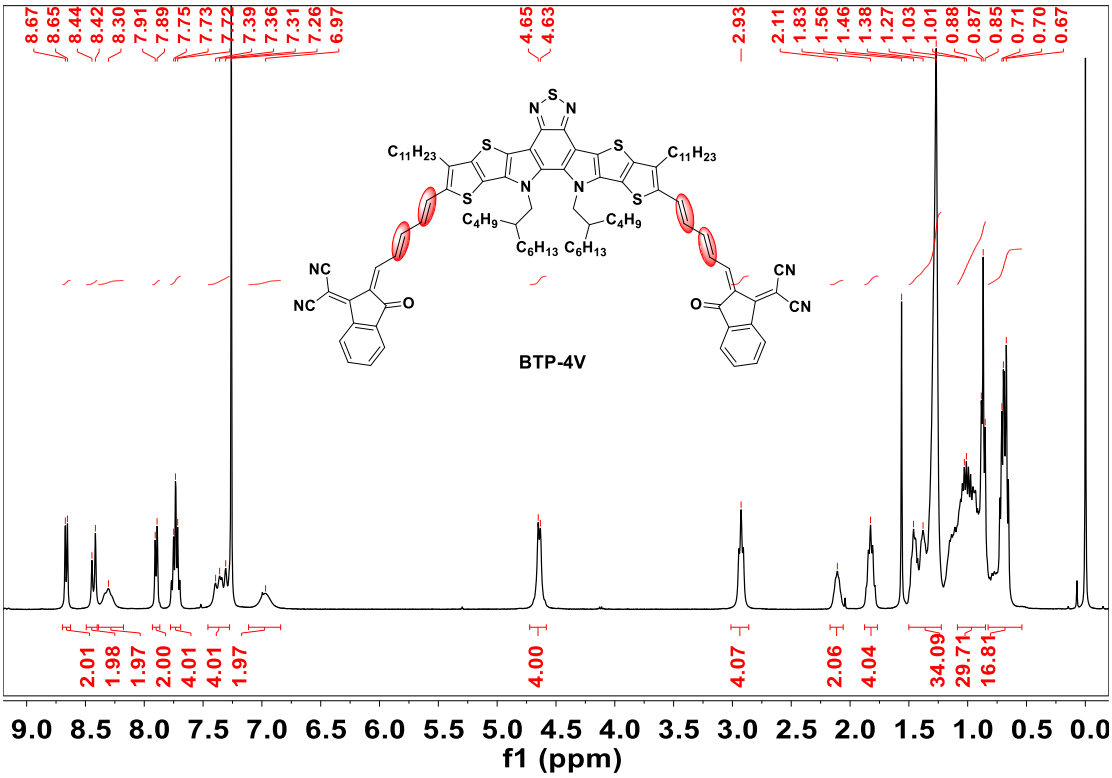

Fig. S15. ^{1}H NMR spectrum of BTP-4V in $CDCl_3$

4. High resolution mass spectra

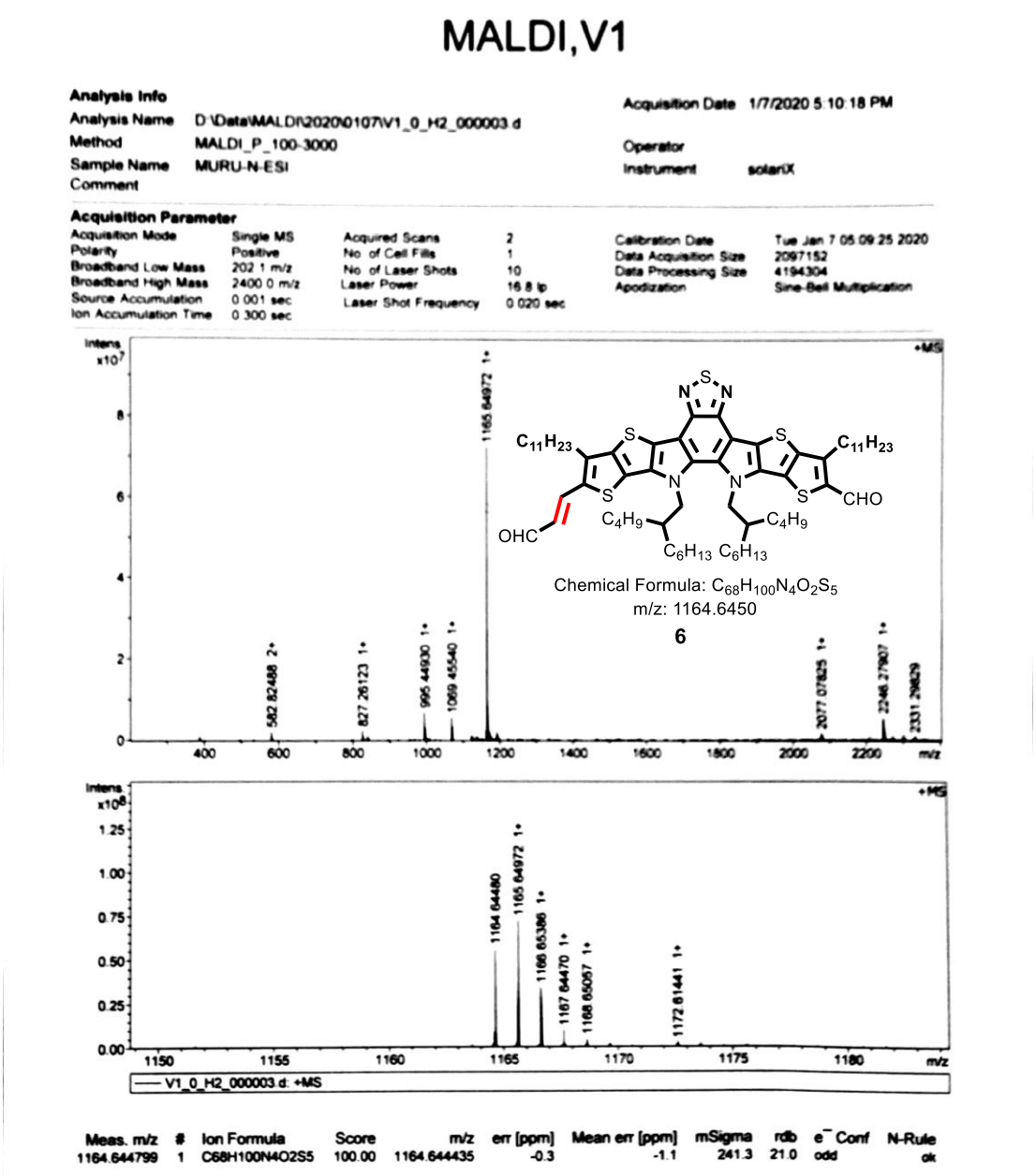

Fig. S16. The MALDI-TOF of compound **6**

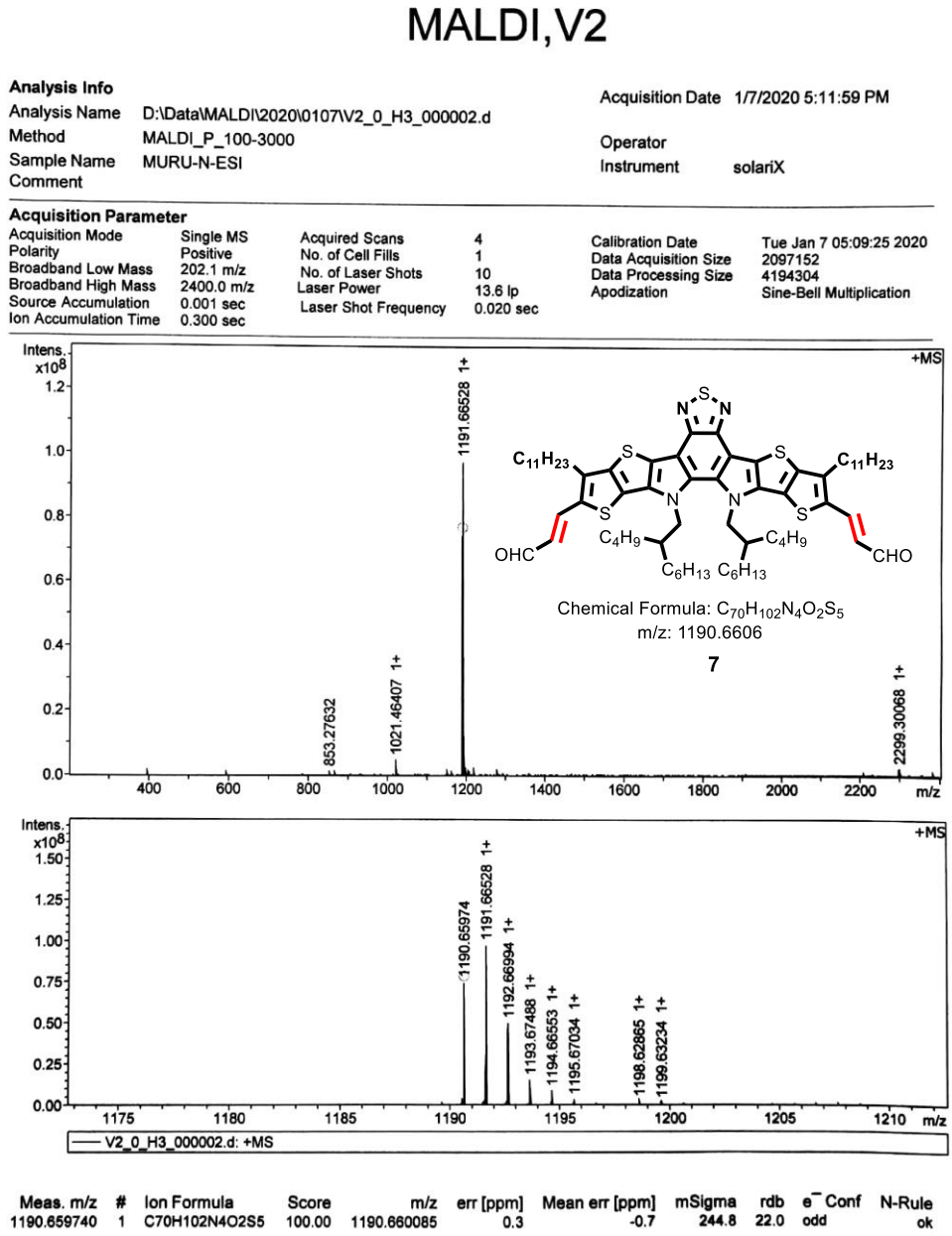

Fig. S17. The MALDI-TOF of compound **7**

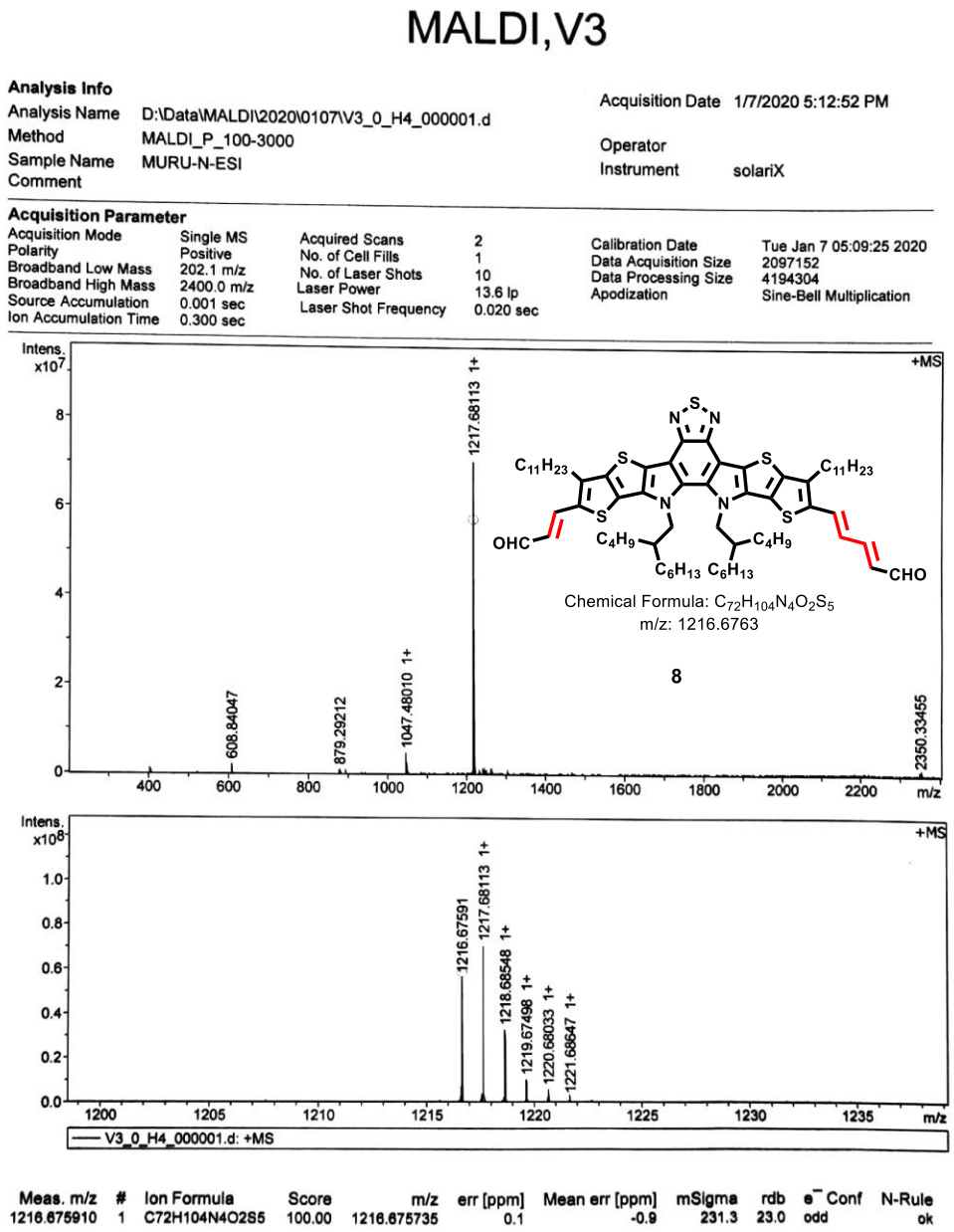

Fig. S18. The MALDI-TOF of compound **8**

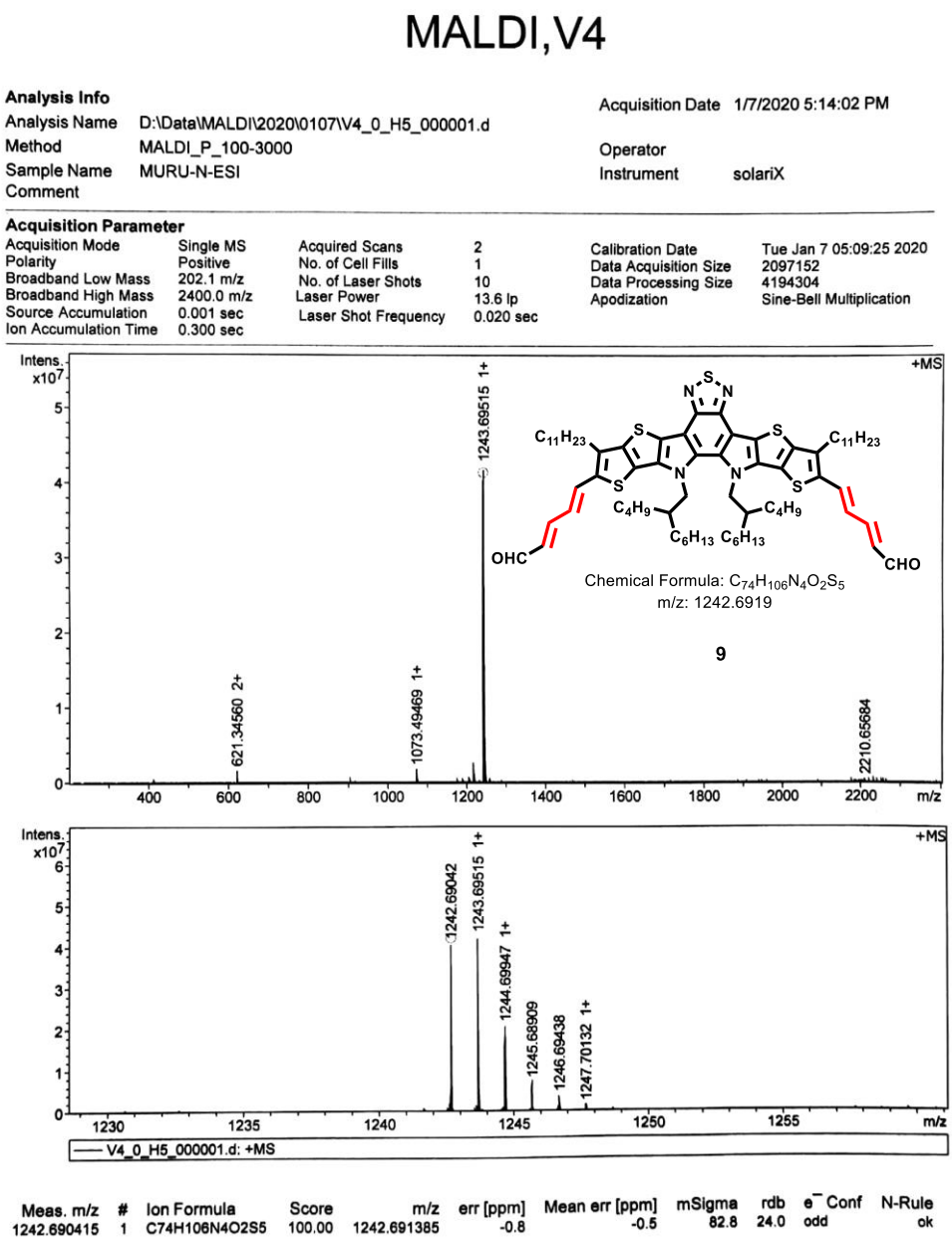

Fig. S19. The MALDI-TOF of compound **9**

MALDI,HJF16

Analysis Info

Analysis Name	D:\Data\MALDI\2020\0107\HJF16_0_H9_000001.d	Acquisition Date	1/7/2020 5:20:30 PM
Method	MALDI_P_100-3000	Operator	
Sample Name	MURU-N-ESI	Instrument	solariX
Comment			

Acquisition Parameter

Acquisition Mode	Single MS	Acquired Scans	2	Calibration Date	Tue Jan 7 05:09:25 2020
Polarity	Positive	No. of Cell Fills	1	Data Acquisition Size	2097152
Broadband Low Mass	202.1 m/z	No. of Laser Shots	10	Data Processing Size	4194304
Broadband High Mass	2600.0 m/z	Laser Power	13.6 lp	Apodization	Sine-Bell Multiplication
Source Accumulation	0.001 sec	Laser Shot Frequency	0.020 sec		
Ion Accumulation Time	0.300 sec				

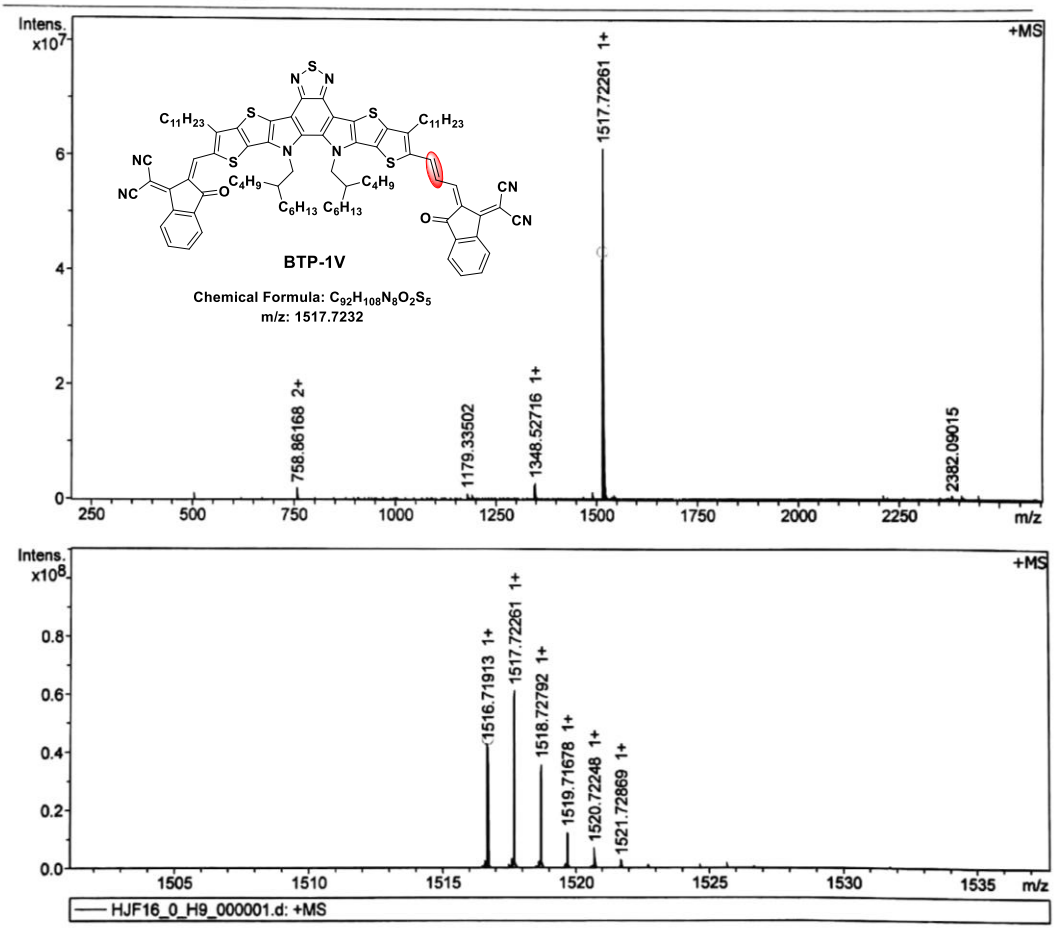

Meas. m/z	#	Ion Formula	Score	m/z	err [ppm]	Mean err [ppm]	mSigma	rdb	e⁻ Conf	N-Rule
1516.719130	1	C92H108N8O2S5	100.00	1516.719331	0.1	-0.5	130.1	43.0	odd	ok

Fig. S20. The MALDI-TOF of BTP-1V

MALDI,HJF7

Analysis Info

Analysis Name	D:\Data\MALDI\2020\0107\HJF7_0_H7_000001.d	Acquisition Date	1/7/2020 5:17:49 PM
Method	MALDI_P_100-3000	Operator	
Sample Name	MURU-N-ESI	Instrument	solariX
Comment			

Acquisition Parameter

Acquisition Mode	Single MS	Acquired Scans	2	Calibration Date	Tue Jan 7 05:09:25 2020
Polarity	Positive	No. of Cell Fills	1	Data Acquisition Size	2097152
Broadband Low Mass	202.1 m/z	No. of Laser Shots	10	Data Processing Size	4194304
Broadband High Mass	2600.0 m/z	Laser Power	13.6 lp	Apodization	Sine-Bell Multiplication
Source Accumulation	0.001 sec	Laser Shot Frequency	0.020 sec		
Ion Accumulation Time	0.300 sec				

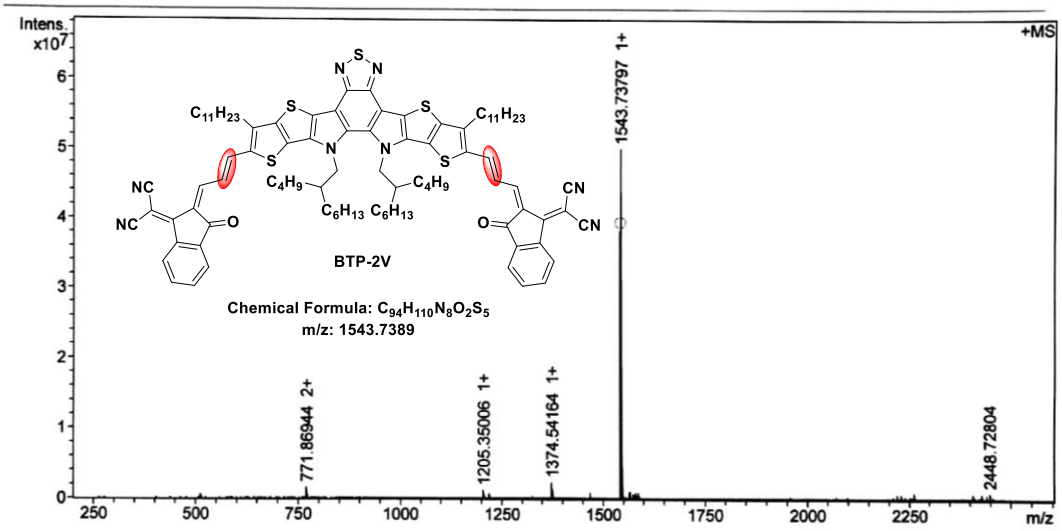

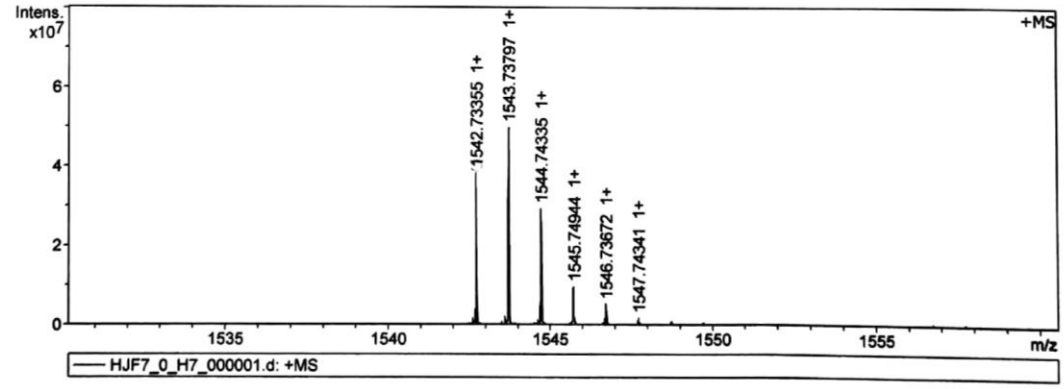

Meas. m/z	#	Ion Formula	Score	m/z	err [ppm]	Mean err [ppm]	mSigma	rdb	e⁻ Conf	N-Rule
1542.733550	1	C94H110N8O2S5	100.00	1542.734981	-0.9	-0.1	121.2	44.0	odd	ok

Fig. S21. MALDI-TOF of BTP-2V

MALDI,HJF15

Analysis Info

Analysis Name	D:\Data\MALDI\2020\0107\HJF15_0_H8_000001.d	Acquisition Date	1/7/2020 5:19:07 PM
Method	MALDI_P_100-3000	Operator	
Sample Name	MURU-N-ESI	Instrument	solariX
Comment			

Acquisition Parameter

Acquisition Mode	Single MS	Acquired Scans	2	Calibration Date	Tue Jan 7 05:09:25 2020
Polarity	Positive	No. of Cell Fills	1	Data Acquisition Size	2097152
Broadband Low Mass	202.1 m/z	No. of Laser Shots	10	Data Processing Size	4194304
Broadband High Mass	2600.0 m/z	Laser Power	13.6 lp	Apodization	Sine-Bell Multiplication
Source Accumulation	0.001 sec	Laser Shot Frequency	0.020 sec		
Ion Accumulation Time	0.300 sec				

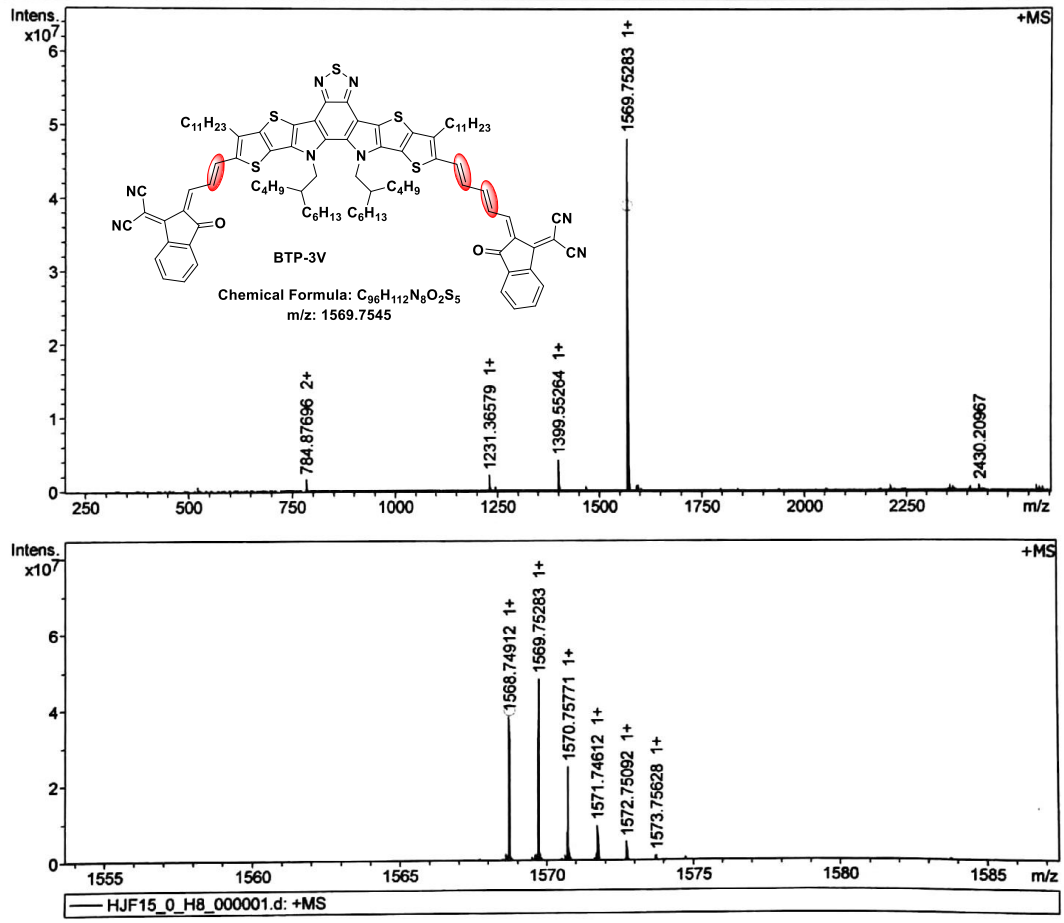

Meas. m/z	#	Ion Formula	Score	m/z	err [ppm]	Mean err [ppm]	mSigma	rdb	e⁻ Conf	N-Rule
1568.749119	1	C96H112N8O2S5	100.00	1568.750631	1.0	0.5	130.1	45.0	odd	ok

Fig. S22. MALDI-TOF of BTP-3V

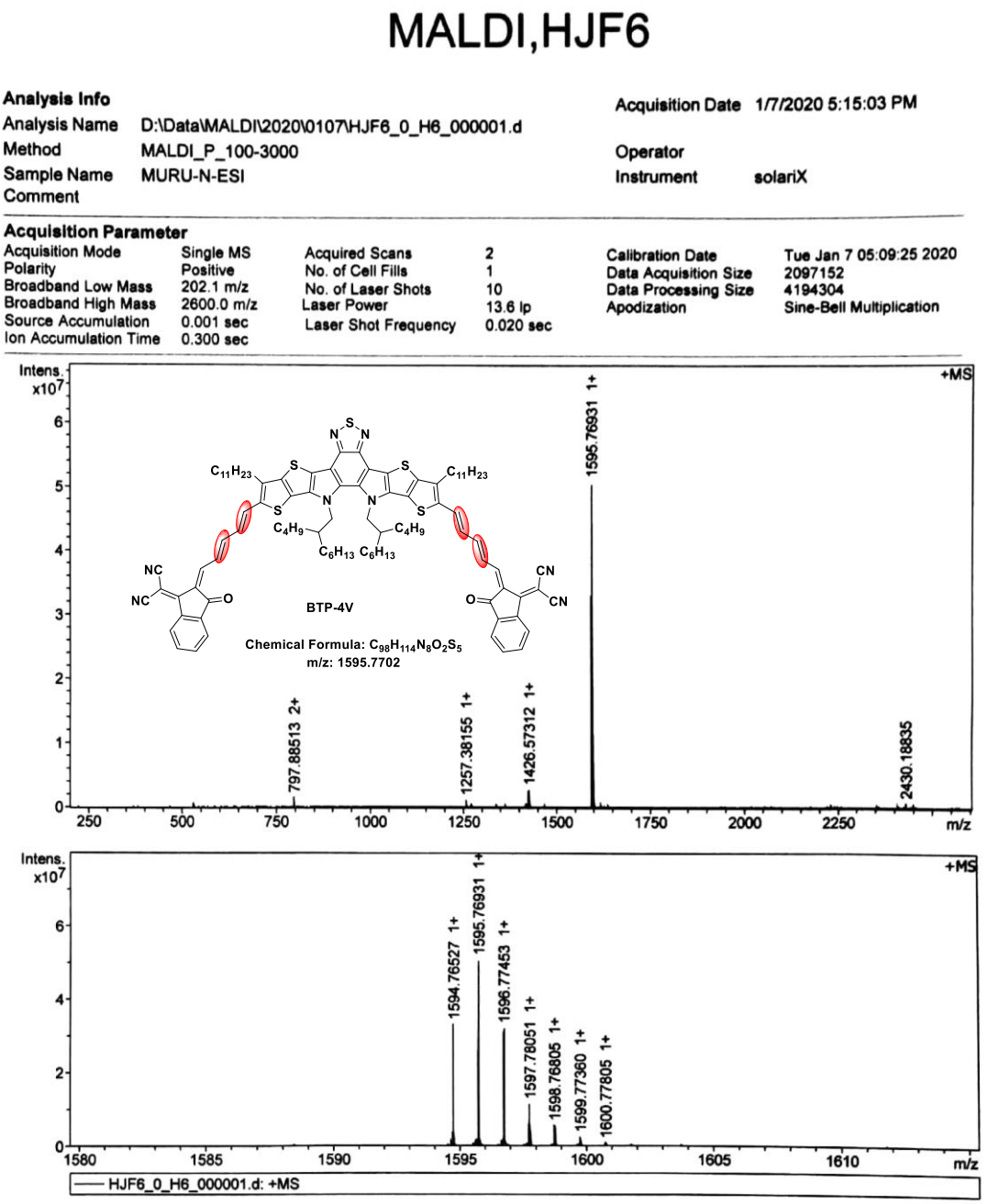

Fig. S23. MALDI-TOF of BTP-4V

5. Uv-vis absorption spectra

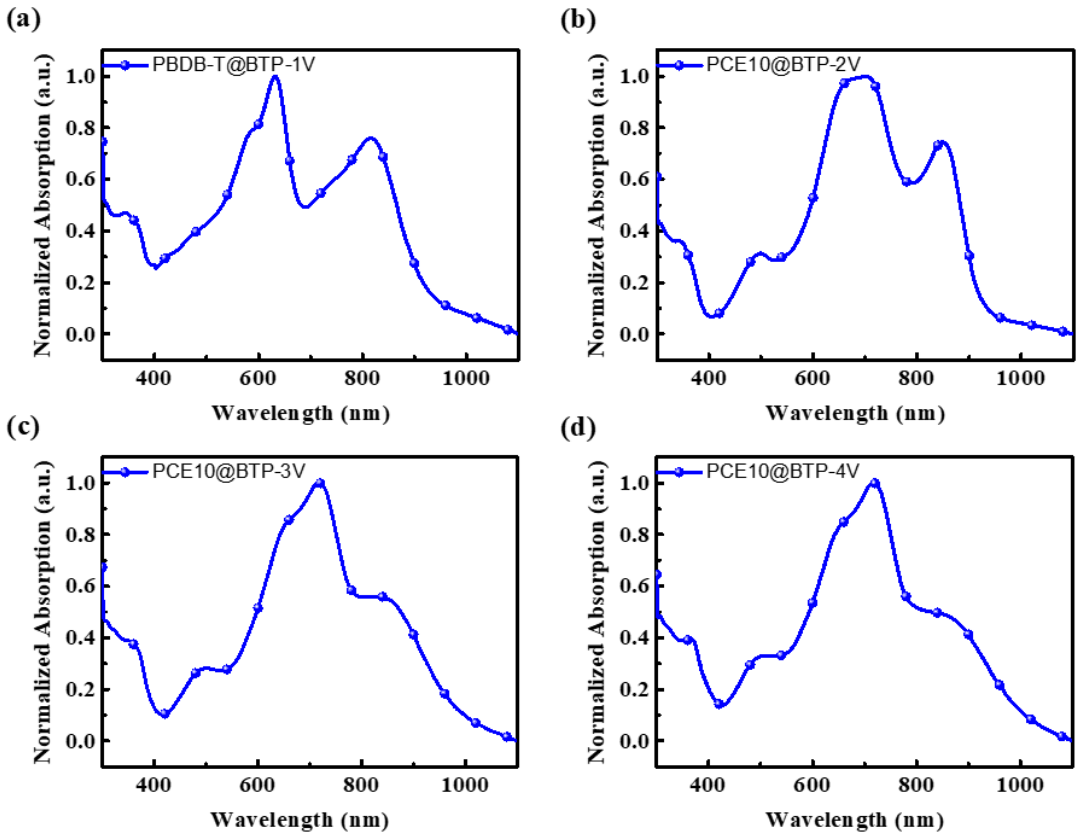

Fig. S24. The absorption spectra of four blend films.

6. photoluminescence (PL) spectra

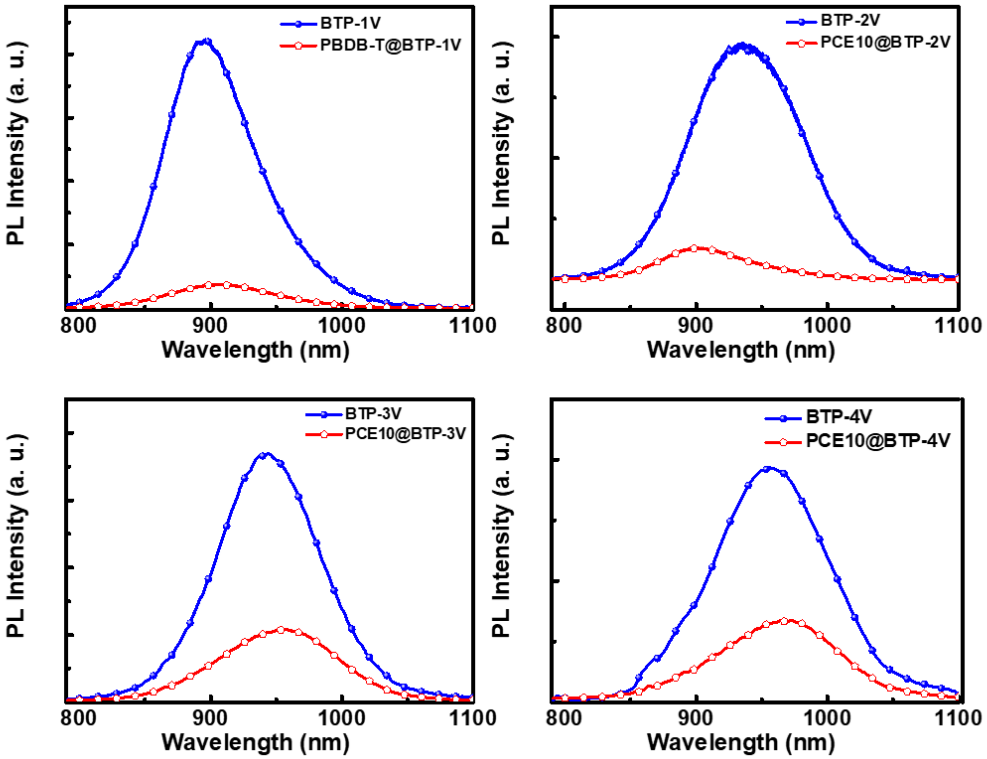

Fig. S25. The photoluminescence (PL) spectra of the neat and blend films

7. Cyclic voltammogram

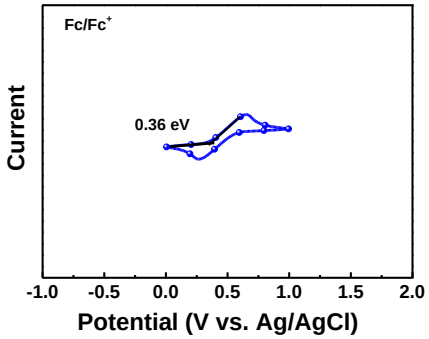

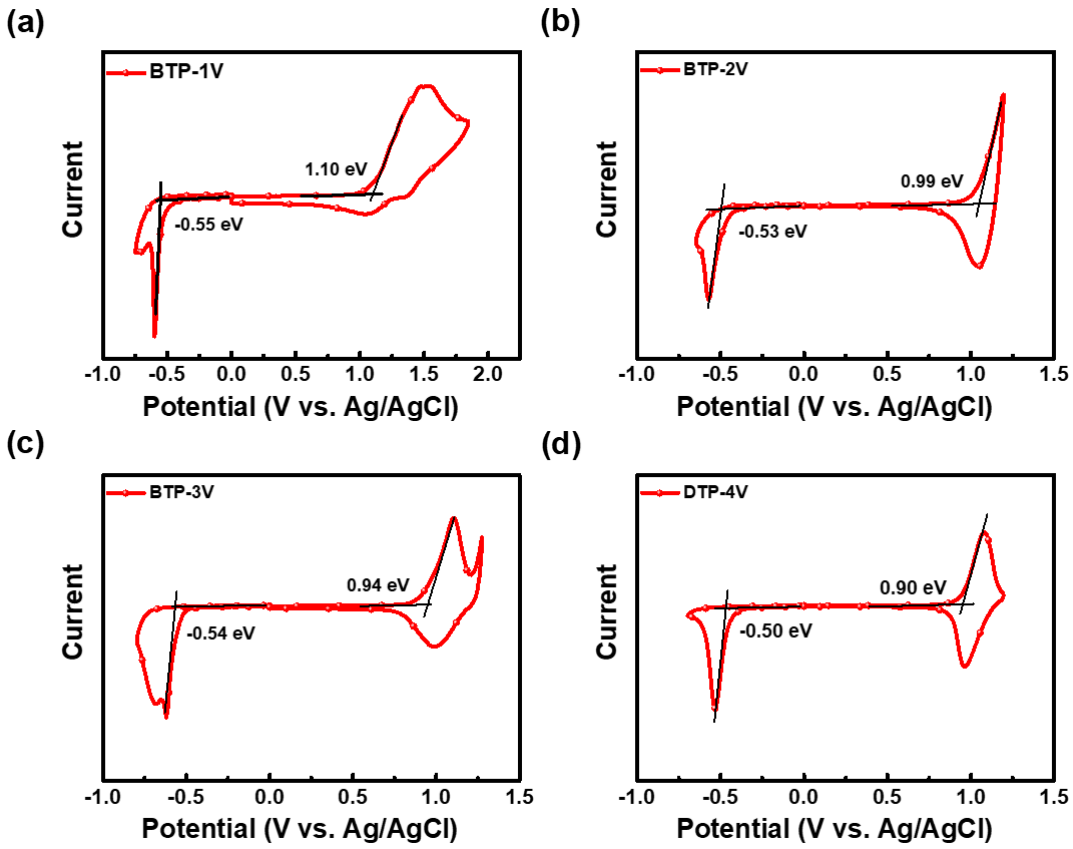

Fig. S26. The cyclic voltammograms of four NFAs in CH_3CN/0.1 M Bu_4NPF_6.

8. Solar cell fabrication and Characterization

Solar cell fabrication and testing. OSCs were made with a device structure of ITO (indium tin oxide)/PEDOT:PSS(poly(3,4-ethylenedioxythiophene): poly (styrene sulfonate))/PBDT-T or PCE10:acceptor/PNDIT-F3N ([(9,9-bis(3'-(N,N-dimethylamino)propyl)-2,7-fluorene)-alt-5,5'-bis(2,2'-thiophene)-2 ,6-naphthalene-1,4,5,8-tetracaboxylic-N,N'-di(2-ethylhexyl)imide])/Ag. The patterned ITO-coated glass was scrubbed by detergent and then cleaned inside an ultrasonic bath by using deionized water, acetone, and isopropyl alcohol sequentially and dried overnight in an oven. Before use, the glass substrates were treated in a UV-Ozone Cleaner for 15 min to improve its work function and clearance. A thin PEDOT: PSS (Heraeus Clevios P VPA 4083) layer was spin-coat onto the ITO substrates at 5000 rpm for 20 s, and then dried at 150°C for 15 min in air. The PEDOT:

PSS coated ITO substrates were transferred to a N_2-filled glove box for further processing. The donor: acceptor blends with a weight ratio of 1:1.2 and a total concentration of 15.4 mg/mL dissolved in chloroform. Then the solution was stirred overnight for intensive mixing in a nitrogen-filled glove box. Then, 0.5% DIO or 1-chloronaphthalene (CN) was added to the chloroform solution 30 minutes before spin coating. The blend solution was spin-cast on the top of PEDOT:PSS layer immediately after being stirred on a hotplate of 55ºC for 30 minutes at 2000 rpm for 30 s. Then the devices were put into vacuum to remove the additive and annealed at 100ºC for 5 min to facilitate phase separation and morphology optimization. A layer of PNDIT-F3Nwas cast onto the processed active layer, and the Ag layer (~100 nm) was deposited in a thermal evaporator under vacuum of 5×10^{-5} Pa through a shadow mask. The current-voltage (*J*-*V*) characteristic curves of all packaged devices were measured by using a Keithley 2400 Source Meter in air. The photocurrent was measured under AM 1.5G (100 mW cm^{-2}) using a Newport solar simulator in an Air. The light intensity was calibrated using a standard Si diode (with KG5 filter, purchased from PV Measurement) to bring spectral mismatch to unity. EQEs were measured using an Enlitech QE-S EQE system equipped with a standard Si diode. Monochromatic light was generated from a Newport 300W lamp source.

EQE measurements. EQEs were measured using an Enlitech QE-S EQE system equipped with a standard Si diode. Monochromatic light was generated from a Newport 300W lamp source.

Hole-mobility measurements. The hole-mobilities were measured using the space charge limited current (SCLC) method, employing a device architecture of ITO/PEDOT:PSS/blend film/MoO_3/Al. The mobilities were obtained by taking current-voltage curves and fitting the results to a space charge limited form, where the SCLC is described by:

$$J = 9\varepsilon_0\varepsilon_r\mu(V_{appl}\text{-}V_{bi}\text{-}V_s)^{2/}8L^3$$

Where ε_0 is the permittivity of free space, ε_r is the relative permittivity of the material

(assumed to be 3), μ is the hole mobility and L is the thickness of the film. Hole mobilities can be found from the plots of $J^{1/2}$ vs V_{appl}-V_{bi}-V_s.

Electron mobility measurements. The electron mobilities were measured using the SCLC method, employing a device architecture of ITO/ZnO/blend film/ PNDIT-F3N/Al. The mobilities were obtained by taking current-voltage curves and fitting the results to a space charge limited form, where the SCLC is described by:

$$J = 9\varepsilon_0\varepsilon_r\mu(V_{appl}\text{-}V_{bi}\text{-}V_s)^{2/}8L^3$$

Where ε_0 is the permittivity of free space, ε_r is the relative permittivity of the material (assumed to be 3), μ is the hole mobility and L is the thickness of the film. Electron mobilities from the plots of $J^{1/2}$ vs V_{appl} -V_{bi}-V_s.

AFM analysis. AFM measurements were performed by using a Scanning Probe Microscope Dimension 3100 in tapping mode. All film samples were spin-cast on ITO substrates.

GIWAXS characterization. GIWAXS measurements were performed at beamline 7.3.3 at the Advanced Light Source. Samples were prepared on Si substrates using identical blend solutions as those used in devices. The 10 keV X-ray beam was incident at a grazing angle of 0.11°-0.15°, which maximized the scattering intensity from the samples. The scattered X-rays were detected using a Dectris Pilatus 2M photon counting detector. In-plane and out-of-plane sector averages were calculated using the Nika software package. The uncertainty for the peak fitting of the GIWAXS data is 0.3 A. The coherence length was calculated using the Scherrer equation:

$$L_c = 2\pi K/\Delta q$$

Where Δq is the full-width at half-maximum of the peak and K is a shape factor (0.94 was used here).

9. Charge recombination and carrier mobility

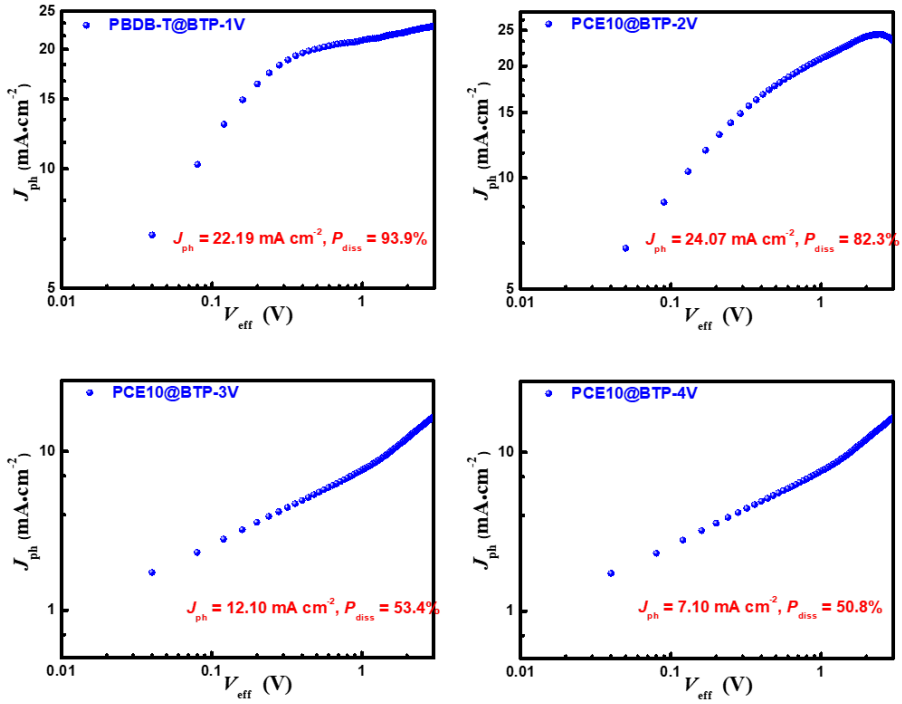

Fig. S27. J_{ph} versus V_{eff} of the optimized devices.

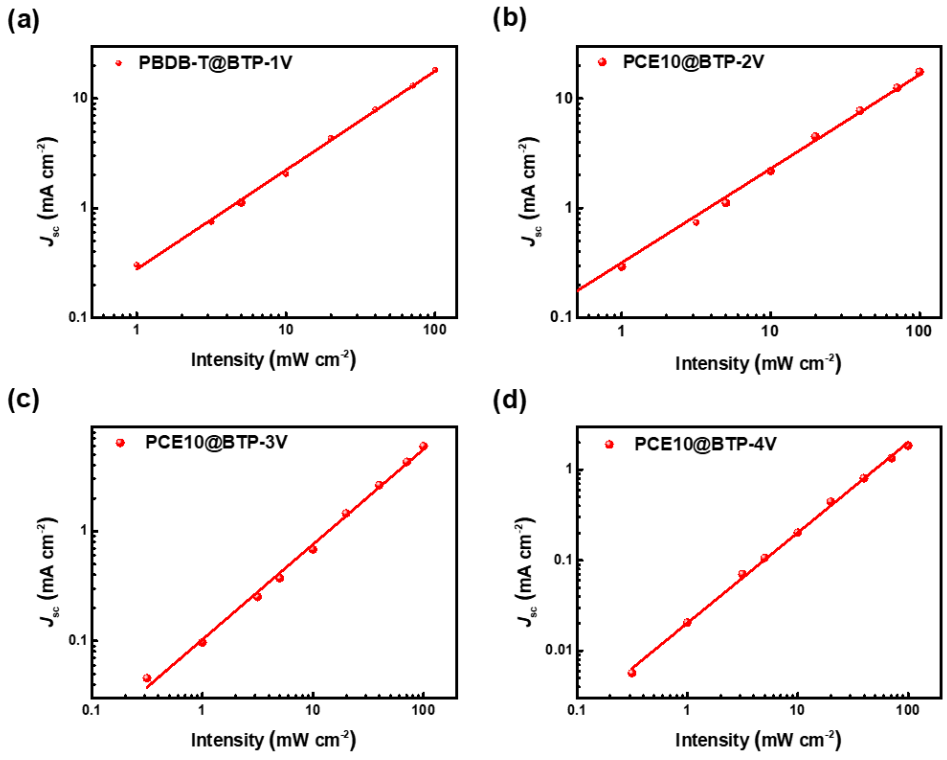

Fig. S28. Light intensity dependency of J_{sc} of the optimized devices.

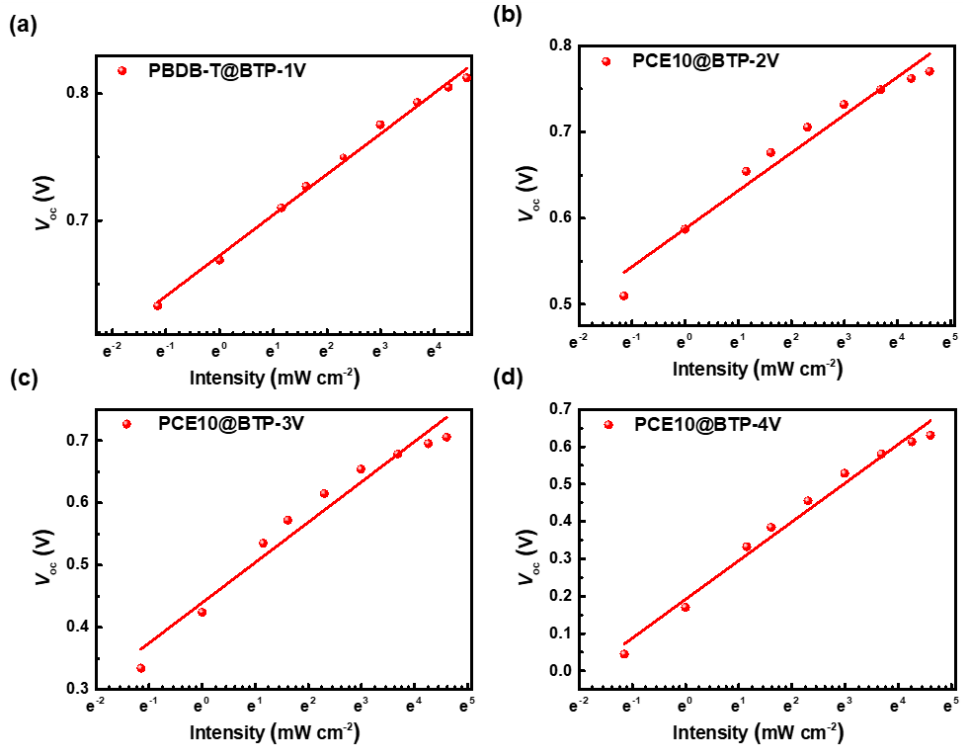

Fig. S29. Light intensity dependency of V_{oc} of the optimized devices.

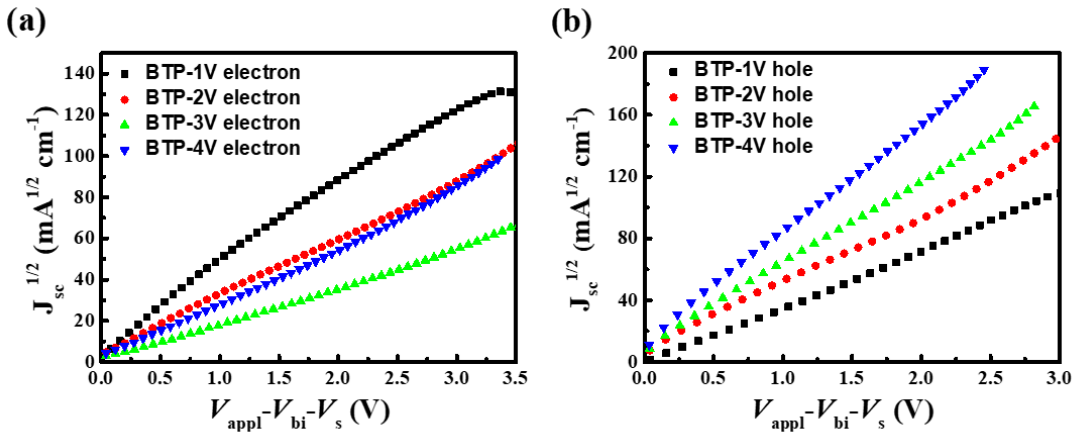

Fig. S30. SCLC characteristics of (a) electron-only and (c) hole-only devices based on four blend films.

10. Eg calculated from UV-vis absorption and PL spectra

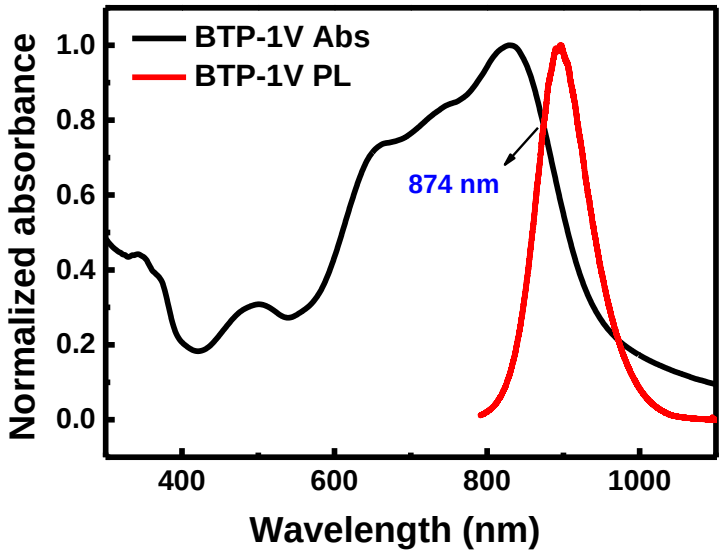

Fig. S31. Normalized UV-vis absorption and PL spectra of BTP-1V.

11. Summary of excellent OSCs based on non-halogenated NFAs with IC end group

Table S1. A summary of reported binary single-junction OSCs based on non-halogenated NFAs with IC end group.

Active layers	E_g^{opt} (eV)	*V*oc (V)	*J*sc (mA/cm^2)	FF (%)	PCE (%)	Reference
FTAZ/IDIC	1.62	0.84	20.8	0.718	12.5	3
PDBT-T1/IC-C1IDT-IC	1.70	0.92	13.39	0.60	7.39	4
J51/ID-Se-IC	1.52	0.91	15.20	0.62	8.6	5
PBDB-T/IDTTIC	1.51	0.92	17.3	0.70	11.2	6
PBDB-T/ITIC-OE	1.57	0.85	14.8	0.67	8.5	7
MP6/IDIC-C4Ph	1.62	0.941	19.06	0.78	14.04	8
J61/SJ-IC	1.49	0.83	16.99	0.66	9.27	9
PBDB-T/ITIC	1.59	0.899	16.81	0.742	11.21	10
PCE10/ITIC-Th	1.60	0.88	20.88	0.713	9.6	11
J61/m-ITIC	1.58	0.91	18.31	0.705	11.77	12
PBDB-T/ITC6-IC	1.60	0.97	16.41	0.73	11.61	13
PFBDB-T/C8-ITIC	1.72	0.94	19.6	0.72	13.2	14
PBDD-T/o-F-ITIC	1.58	0.918	18.07	0.67	11.11	16
PBDTTT-E-T/IEICO	1.34	0.80	18.55	0.62	9.19	17

PBDB-T/6(IDT-3MT)	1.52	0.95	14.43	0.613	8.40	18
PBDB-T/IDT-Tz	1.66	0.88	13.67	0.708	8.52	19
PBDB-T/IDT-BOC6	1.63	1.01	17.52	0.54	9.6	20
FTAZ/ITIC-Th-O/IDIC	1.40	0.85	18.5	0.719	11.6	21
P3HT/TrBTIC	1.80	0.88	13.04	0.719	8.25	22
PBDB-T/DF-PCIC	1.59	0.91	15.66	0.72	10.14	23
PBT1-C/TPTT-IC	1.63	0.96	15.6	0.70	10.5	24
PBDB-T/ITDI	1.53	0.94	13.94	0.598	8.00	25
PBDB-T/FTIC-C6C8	1.63	0.93	18.55	0.65	11.12	26
PBDB-T/FDICTF	1.63	0.94	15.81	0.66	10.06	27
PBDB-T/DTCCIC-C17	1.60	0.97	14.27	0.67	9.48	28
PCE10/DTCC-IC	1.59	0.95	11.23	0.56	6.0	29
PBDB-T/DTCFOIC	1.69	1.00	11.93	0.579	6.92	30
J71/H2FCN-C16	1.59	0.90	18.62	0.66	11.18	31
HFQx-T/BZIC	1.45	0.84	12.67	0.59	6.3	32
PBDB-T/Y1	1.44	0.87	22.44	0.691	13.42	33
PBDB-T/Y9	1.36	0.90	23.28	0.63	13.26	34
PBDB-T/Y5	1.38	0.88	22.8	0.702	14.1	35
PCE10/6TIC	1.30	0.74	19.22	0.541	8.13	36
PCE10/4TIC	1.26	0.70	14.58	0.487	5.26	36
PBDB-T /BTP-1V	**1.28**	**0.84**	**20.86**	**0.63**	**11.03**	**This work**
PCE10/BTP-2V	**1.28**	**0.77**	**19.80**	**0.51**	**7.87**	**This work**

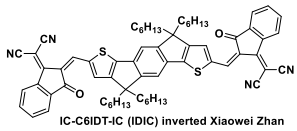

IC-C6IDT-IC (IDIC) inverted Xiaowei Zhan

PDBT-T1:IC-C6IDT-IC 1:1

HOMO = -5.69 eV, LUMO = -3.91 eV, E_g^{opt} = 1.62 eV

J_{sc} = 15.05 mA cm^{-2} ; V_{oc} = 0.89 V; FF = 0.63;

PCE = 8.71%, J. Am. Chem. Soc., 2016, 138, 2973-2976

9.2% Adv. Energy Mater. 2016, 1600854 inverted

12.5% FTAZ:IDIC Adv. Mater. 2018, 1706363 inverted

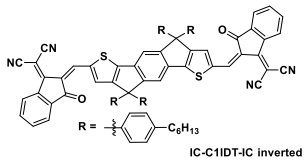

IC-C1IDT-IC inverted Xiaowei Zhan

PDBT-T1:IC-C1IDT-IC 1:1

HOMO = -5.91 eV, LUMO = -3.83 eV, E_g^{opt} = 1.70 eV

J_{sc} = 13.39 mA cm^{-2} ; V_{oc} = 0.92 V; FF = 0.60;

PCE = 7.39%, Adv. Energy Mater. 2016, 1600854

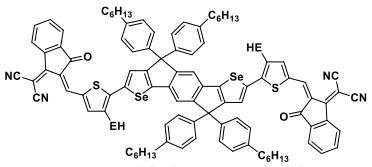

ID-Se-IC normal device Liang-Sheng Liao

J51:ID-Se-IC 1:1

HOMO = -5.45 eV, LUMO = -3.79 eV, E_g^{opt} = 1.52 eV,

J_{sc} = 15.20 mA cm^{-2} ; V_{oc} = 0.91 V; FF = 0.62;

PCE = 8.6%, Energy Environ. Sci., 2016, 9, 3429-3435

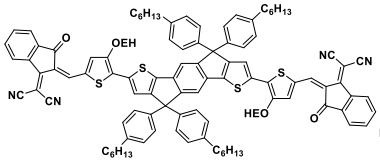

IEICO tandem device Jianhui Hou

PBDD4T-2F:$PC_{71}BM$ (Front Cell) & PBDTTT-E-T:IEICO(rare cell)

HOMO = -5.32 eV, LUMO = -3.95 eV, E_g^{opt} = 1.34 eV,

J_{sc} = 11.51 mA cm^{-2} ; V_{oc} = 1.71 V; FF = 0.66;

PCE = 12.80% Adv. Mater. 2017, 1606340

PCE = 10.7% Adv. Mater. 2016, 28, 8283-8287 tandem

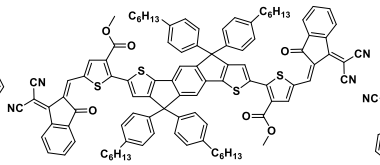

6(IDT-3MT) inverted device Dong Hoon Choi

PBDB-T: 6(IDT-3MT) 1:1

HOMO = -5.68 eV, LUMO = -4.16 eV, E_g^{opt} = 1.52 eV,

J_{sc} = 14.43 mA cm^{-2} ; V_{oc} = 0.95 V; FF = 0.613;

PCE = 8.40%, J. Mater. Chem. C, 2018, 6, 7549-7556

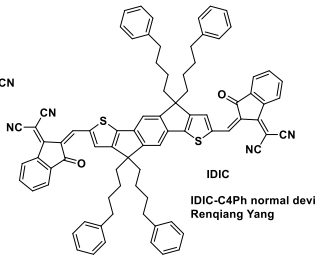

IDIC

IDIC-C4Ph normal device Renqiang Yang

MP6:IDIC-C4Ph 1:1

HOMO = -5.70 eV, LUMO = -3.93 eV, E_g^{opt} = 1.62 eV

J_{sc} = 19.06 mA cm^{-2} ; V_{oc} = 0.941 V; FF = 0.7832;

PCE = 14.04%, Adv. Mater. 2019, 1807832

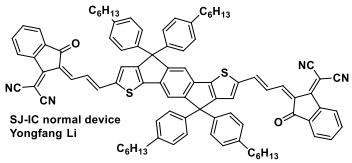

SJ-IC normal device Yongfang Li

J61:SJ-IC 1:1

HOMO = -5.61 eV, LUMO = -3.94 eV, E_g^{opt} = 1.49 eV,

J_{sc} = 16.99 mA cm^{-2} ; V_{oc} = 0.83 V; FF = 0.659;

PCE = 9.27% J. Mater. Chem. A, 2017,5, 22588-22597

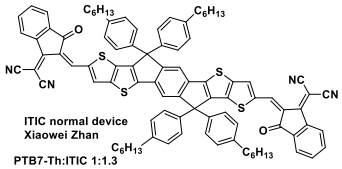

ITIC normal device Xiaowei Zhan

PTB7-Th:ITIC 1:1.3

HOMO = -5.48 eV, LUMO = -3.83 eV, E_g^{opt} = 1.59 eV

J_{sc} = 14.21 mA cm^{-2} ; V_{oc} = 0.81 V; FF = 0.591;

PCE = 6.8% Adv. Mater. 2015, 27, 1170-1174

11.2% PBDB-T@ITIC Adv. Mater. 2016, 28, 4734-4739

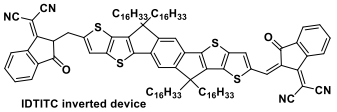

IDTITC inverted device

PBDB-T:IDTTIC 1:1

HOMO = -5.68 eV, LUMO = -3.89 eV, E_g^{opt} = 1.51 eV

J_{sc} = 17.3 mA cm^{-2} ; V_{oc} = 0.919 V; FF = 0.704;

PCE = 11.2%, Adv. Funct. Mater. 2018, 1802895

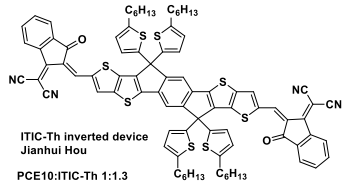

ITIC-Th inverted device Jianhui Hou

PCE10:ITIC-Th 1:1.3

HOMO = -5.66 eV, LUMO = -3.93 eV, E_g^{opt} = 1.60 eV

J_{sc} = 20.88 mA cm^{-2} ; V_{oc} = 0.88 V; FF = 0.713;

PCE = 9.6%, J. Am. Chem. Soc. 2016, 138, 4955-4961

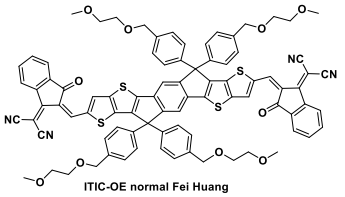

ITIC-OE normal Fei Huang

PBDB-T:ITIC-OE 1:1

HOMO = -5.67 eV, LUMO = -4.03 eV, E_g^{opt} = 1.57 eV

J_{sc} = 14.8 mA cm^{-2} ; V_{oc} = 0.85 V; FF = 0.67;

PCE = 8.5%, J. Mater. Chem. A, 2018, , 395-403

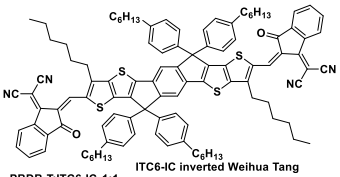

ITC6-IC inverted Weihua Tang

PBDB-T:ITC6-IC 1:1

HOMO = -5.73 eV, LUMO = -3.92 eV, E_g^{opt} = 1.60 eV,

J_{sc} = 16.41 mA cm^{-2}; V_{oc} = 0.97 V; FF = 0.73;

PCE = 11.61%, Adv. Funct. Mater. 2018, 1705095

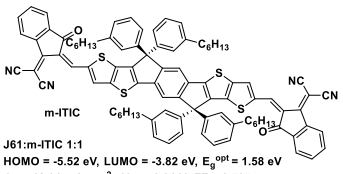

m-ITIC

J61:m-ITIC 1:1

HOMO = -5.52 eV, LUMO = -3.82 eV, E_g^{opt} = 1.58 eV

J_{sc} = 18.31 mA cm^{-2} ; V_{oc} = 0.91 V; FF = 0.705;

PCE = 11.77%, J. Am. Chem. Soc. 2016, 138, 15011-15018

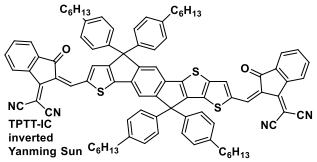

TPTT-IC inverted Yanming Sun

PBT1-C:TPTT-IC 1:1 M_n 25.5 PDI 1.76

HOMO = -5.78 eV, LUMO = -3.95 eV, E_g^{opt} = 1.63 eV

J_{sc} = 15.6 mA cm^{-2} ; V_{oc} = 0.96 V; FF = 0.70;

PCE = 10.5%, J. Mater. Chem. C, 2018, 6, 4873--4877

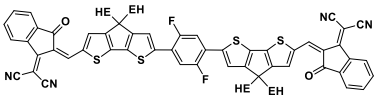

DF-PCIC inverted Hongzheng Chen

PBDB-T:DF-PCIC 1:1.2

HOMO = -5.49 eV, LUMO = -3.77 eV, E_g^{opt} = 1.59 eV

J_{sc} = 15.66 mA cm^{-2} ; V_{oc} = 0.91 V; FF= 0.72

PCE = 10.14% Adv. Mater. 2017, 1705208

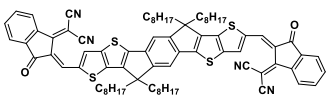

C8-ITIC inverted device Martin Heeney

PFBDB-T:C8-ITIC 1:1.25

HOMO = -5.63 eV, LUMO = -3.91 eV, E_g^{opt} = 1.72 eV

J_{sc} = 19.6 mA cm^{-2} ; V_{oc} = 0.94 V; FF = 0.72;

PCE = 13.2% Adv. Mater. 2018, 30, 1705209

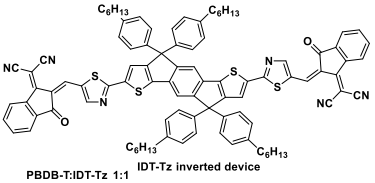

IDT-Tz inverted device

PBDB-T:IDT-Tz 1:1

HOMO = -5.62 eV, LUMO = -3.96 eV, E_g^{opt} = 1.66 eV,

J_{sc} = 13.67 mA cm^{-2} ; V_{oc} = 0.88 V; FF = 0.708;

PCE = 8.52% J. Mater. Chem. A, 2017, 5 , 21674-21678

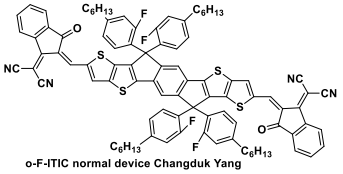

o-F-ITIC normal device Changduk Yang

PBDD-T:o-F-ITIC 1.3:1

HOMO = -5.66 eV, LUMO = -3.94 eV, E_g^{opt} = 1.58 eV

J_{sc} = 18.07 mA cm^{-2} ; V_{oc} = 0.918 V; FF = 0.670;

PCE = 11.11% J. Mater. Chem. A, 2019, 7, 18468-18479

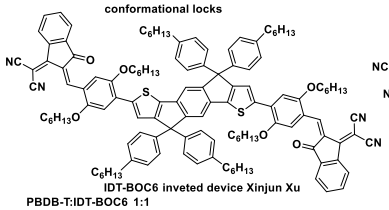

IDT-BOC6 inveted device Xinjun Xu

PBDB-T:IDT-BOC6 1:1
HOMO = -5.51 eV, LUMO = -3.78 eV, E_g^{opt} = 1.63 eV
J_{sc} = 17.52 mA cm^{-2} ; V_{oc} =1.01 V; FF = 0.54;
PCE = 9.6%, J. Am. Chem. Soc. 2017, 139, 3356-3359

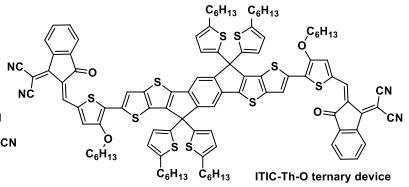

ITIC-Th-O ternary device

FTAZ:ITIC-Th-O:IDIC
HOMO = -5.35 eV, LUMO = -3.91 eV, E_g^{opt} = 1.40 eV,
J_{sc} = 18.5 mA cm^{-2} ; V_{oc} = 0.85 V; FF = 0.719;
PCE = 11.6%, Adv. Mater. 2018, 1801501

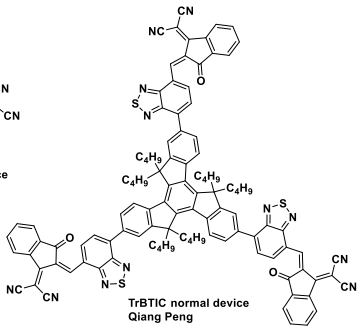

TrBTIC normal device
Qiang Peng

P3HT:TrBTIC 1:1.2 aging 40 min
HOMO = -5.56 eV, LUMO = -3.62 eV, E_g^{opt} = 1.80 eV
J_{sc} = 13.04 mA cm^{-2} ; V_{oc} = 0.88 V; FF = 0.719;
PCE = 8.25%, Adv. Mater. 2019, 31, 1906045

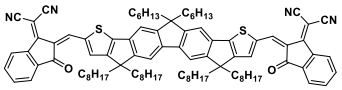

FTIC-C6C8 inverted device Zhishan Bo

PBDB-T:FTIC-C6C8 1:1
HOMO = -5.64 eV, LUMO = -4.01 eV, E_g^{opt} = 1.63 eV
J_{sc} = 18.55 mA cm^{-2} ; V_{oc} = 0.93 V; FF = 0.6472;
PCE = 11.12%, J. Mater. Chem. A, 2017, 5 , 7776-7783

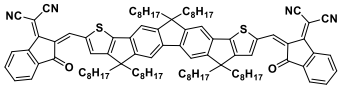

FDICTF conventional Yongsheng Chen

PBDB-T:FDICTF 1:1.2
HOMO = -5.43 eV, LUMO = -3.71 eV, E_g^{opt} = 1.63 eV
J_{sc} = 15.81 mA cm^{-2} ; V_{oc} = 0.94 V; FF = 0.66;
PCE = 10.06%, Adv. Mater. 2016, 201604964

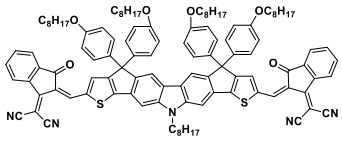

DTCC-IC normal Yanming Sun

PTB7-Th:DTCC-IC 1:1
HOMO = -5.50 eV, LUMO = -3.87 eV, E_g^{opt} = 1.59 eV
J_{sc} = 11.23 mA cm^{-2} ; V_{oc} = 0.95 V; FF = 0.562;
PCE = 6.0%, J. Mater. Chem. A, 2017, 5 , 7451-7461

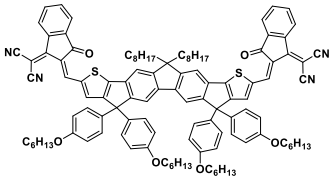

DTCFOIC inverted ternary Ping Shen

PBDB-T:$PC_{71}BM$:DTCFOIC 1:1.5:0.2
HOMO = -5.63 eV, LUMO = -3.93 eV, E_g^{opt} = 1.69 eV,
J_{sc} = 18.56 mA cm^{-2} ; V_{oc} = 0.88 V; FF = 0.641;
PCE = 10.41%, J. Mater. Chem. A, 2018, 6 , 20313-20326
PBDB-T:DTCFOIC 6.92% binary device

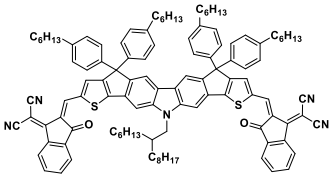

H2FCN-C16 inverted device
Qingdong Zheng

J71:H2FCN-C16 1:1
HOMO = -5.95 eV, LUMO = -3.99 eV, E_g^{opt} = 1.59 eV,
J_{sc} = 18.62 mA cm^{-2} ; V_{oc} = 0.90 V; FF = 0.66;
PCE = 11.18%, Chem. Mater. 2019, 31, 5953-5963

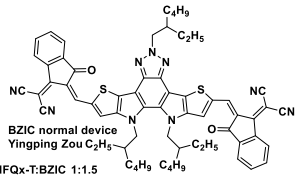

BZIC normal device
Yingping Zou

HFQx-T:BZIC 1:1.5
HOMO = -5.42 eV, LUMO = -3.88 eV, E_g^{opt} = 1.45 eV
J_{sc} = 12.67 mA cm^{-2} ; V_{oc} = 0.84 V; FF = 0.59;
PCE = 6.3%, ACS Appl. Mater. Interfaces 2017, 9, 31985-31992

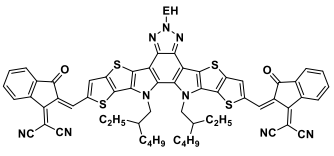

Y1 inverted device Yingping Zou

PBDB-T:Y1 1:1
HOMO = -5.45 eV, LUMO = -3.95 eV, E_g^{opt} = 1.44 eV
J_{sc} = 22.44 mA cm^{-2} ; V_{oc} = 0.87 V; FF = 0.691;
PCE = 13.42%, Nature Communications, 2019,10(1): 570

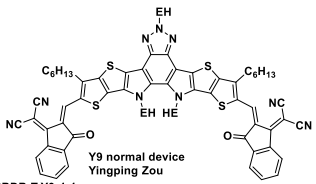

Y9 normal device
Yingping Zou

PBDB-T:Y9 1:1
HOMO = -5.59 eV, LUMO = -3.78 eV, E_g^{opt} = 1.36 eV
J_{sc} = 23.28 mA cm^{-2} ; V_{oc} = 0.90 V; FF = 0.63;
PCE = 13.26%, Journal of Energy Chemistry 2020,42,169-173

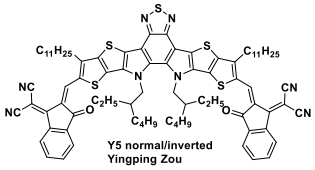

Y5 normal/inverted
Yingping Zou

PBDB-T:Y5 1:1.5
HOMO = -5.55 eV, LUMO = -3.87 eV, E_g^{opt} = 1.38 eV
J_{sc} = 22.8 mA cm^{-2} ; V_{oc} = 0.88 V; FF = 0.702;
PCE = 14.1%, Adv. Mater. 2019, 1807577
J61:Y5 11.3%, TTFQx-T1:Y5 13.1%,

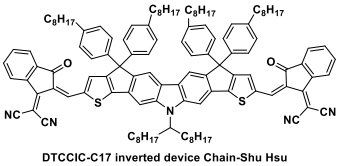

DTCCIC-C17 inverted device Chain-Shu Hsu

PBDB-T:DTCCIC-C17 1:1.5
HOMO = -5.46 eV, LUMO = -3.65 eV, E_g^{opt} = 1.60 eV
J_{sc} = 14.27 mA cm^{-2} ; V_{oc} = 0.97 V; FF = 0.67;
PCE = 9.48%, ACS Appl. Mater. Interfaces 2017, 9, 42035-42042

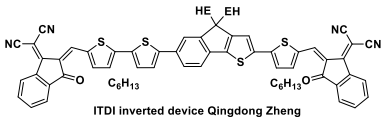

ITDI inverted device Qingdong Zheng

PBDB-T:ITDI 1:1
HOMO = -5.89 eV, LUMO = -4.18 eV, E_g^{opt} = 1.53 eV
J_{sc} = 13.94 mA cm^{-2} ; V_{oc} = 0.94 V; FF = 0.5978;
PCE = 8.00%, ACS Appl. Mater. Interfaces 2017, 9, 24771-24777

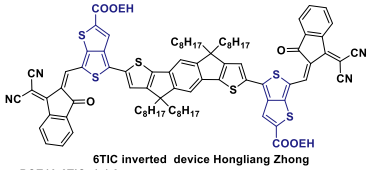

6TIC inverted device Hongliang Zhong

PCE10:6TIC 1:1.3
HOMO = -5.34 eV, LUMO = -3.96 eV, E_g^{opt} = 1.30 eV
J_{sc} = 19.22 mA cm^{-2} ; V_{oc} = 0.74 V; FF = 0.541;
PCE = 8.13%, J. Mater. Chem. C, 2020, 8, 4357-4364

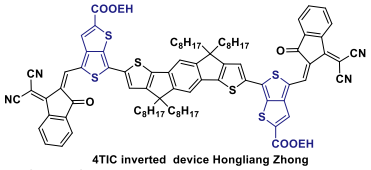

4TIC inverted device Hongliang Zhong

PCE10:4TIC 1:1.3
HOMO = -5.36 eV, LUMO = -4.11 eV, E_g^{opt} = 1.26 eV
J_{sc} = 14.58 mA cm^{-2} ; V_{oc} = 0.70 V; FF = 0.487;
PCE = 5.26%, J. Mater. Chem. C, 2020, 8, 4357-4364

12. References

1. J. Yuan, Y. Zhang, L. Zhou, G. Zhang, H.-L. Yip, T.-K. Lau, X. Lu, C. Zhu, H. Peng, P. A.

Johnson, M. Leclerc, Y. Cao, J. Ulanski, Y. Li and Y. Zou, *Joule*, 2019, 3, 1140-1151.
2. K. Jiang, Q. Wei, J. Y. L. Lai, Z. Peng, H. K. Kim, J. Yuan, L. Ye, H. Ade, Y. Zou and H. Yan, *Joule*, 2019, 3, 3020-3033.
3. Y. Lin, F. Zhao, S. K. K. Prasad, J.-D. Chen, W. Cai, Q. Zhang, K. Chen, Y. Wu, W. Ma, F. Gao, J.-X. Tang, C. Wang, W. You, J. M. Hodgkiss and X. Zhan, *Advanced Materials*, 2018, 30, 1706363.
4. Y. Lin, T. Li, F. Zhao, L. Han, Z. Wang, Y. Wu, Q. He, J. Wang, L. Huo, Y. Sun, C. Wang, W. Ma and X. Zhan, *Advanced Energy Materials*, 2016, 6, 1600854.
5. Y. Li, L. Zhong, F.-P. Wu, Y. Yuan, H.-J. Bin, Z.-Q. Jiang, Z. Zhang, Z.-G. Zhang, Y. Li and L.-S. Liao, *Energy & Environmental Science*, 2016, 9, 3429-3435.
6. X. Song, N. Gasparini, M. M. Nahid, H. Chen, S. M. Macphee, W. Zhang, V. Norman, C. Zhu, D. Bryant, H. Ade, I. McCulloch and D. Baran, *Advanced Functional Materials*, 2018, 0, 1802895.
7. C. Duan, X. Liu, B. Xie, Z. Wang, B. Fan, K. Zhang, B. Lin, F. Colberts, W. Ma, R. A. J. Janssen, F. Huang and Y. Cao, *Journal of Materials Chemistry A*, 2017, 6, 395-403.
8. Y. Li, N. Zheng, L. Yu, S. Wen, C. Gao, M. Sun and R. Yang, *Advanced Materials*, 2019, DOI: doi:10.1002/adma.201807832, 1807832.
9. X. Li, T. Yan, H. Bin, G. Han, L. Xue, F. Liu, Y. Yi, Z.-G. Zhang, T. P. Russell and Y. Li, *Journal of Materials Chemistry A*, 2017, 5, 22588-22597.
10. W. Zhao, D. Qian, S. Zhang, S. Li, O. Inganäs, F. Gao and J. Hou, *Advanced Materials*, 2016, 28, 4734-4739.
11. Y. Lin, F. Zhao, Q. He, L. Huo, Y. Wu, T. C. Parker, W. Ma, Y. Sun, C. Wang, D. Zhu, A. J. Heeger, S. R. Marder and X. Zhan, *Journal of the American Chemical Society*, 2016, 138, 4955-4961.
12. Y. Yang, Z.-G. Zhang, H. Bin, S. Chen, L. Gao, L. Xue, C. Yang and Y. Li, *Journal of the American Chemical Society*, 2016, 138, 15011-15018.
13. Z. Zhang, J. Yu, X. Yin, Z. Hu, Y. Jiang, J. Sun, J. Zhou, F. Zhang, T. P. Russell, F. Liu and W. Tang, *Advanced Functional Materials*, 2018, 28, 1705095.
14. Z. Fei, F. D. Eisner, X. Jiao, M. Azzouzi, J. A. Röhr, Y. Han, M. Shahid, A. S. R. Chesman, C. D. Easton, C. R. McNeill, T. D. Anthopoulos, J. Nelson and M. Heeney, *Advanced Materials*, 2018, 30, 1705209.
15. X. Liu, X. Wang, Y. Xiao, Q. Yang, X. Guo and C. Li, *Advanced Energy Materials*, 2020, DOI: 10.1002/aenm.201903650, 1903650.
16. J. Lee, E. M. Go, S. Dharmapurikar, J. Xu, S. M. Lee, M. Jeong, K. C. Lee, J. Oh, Y. Cho, C. Zhang, M. Xiao, S. K. Kwak and C. Yang, *Journal of Materials Chemistry A*, 2019, 7, 18468-18479.
17. H. Yao, Y. Chen, Y. Qin, R. Yu, Y. Cui, B. Yang, S. Li, K. Zhang and J. Hou, *Advanced Materials*, 2016, 28, 8283-8287.
18. S. H. Park, G. E. Park, S. Choi, Y. U. Kim, S. Y. Park, C. G. Park, M. J. Cho and D. H. Choi, *Journal of Materials Chemistry C*, 2018, 6, 7549-7556.
19. S. Yu, Y. Chen, L. Yang, P. Ye, J. Wu, J. Yu, S. Zhang, Y. Gao and H. Huang, *Journal of Materials Chemistry A*, 2017, 5, 21674-21678.
20. Y. Liu, Z. Zhang, S. Feng, M. Li, L. Wu, R. Hou, X. Xu, X. Chen and Z. Bo, *Journal of the American Chemical Society*, 2017, 139, 3356-3359.

21. C. Pei, W. Jiayu, Z. Qianqian, H. Wenchao, Z. Jingshuai, W. Rui, C. Sheng-Yung, S. Pengyu, M. Lei, Z. Hongxiang, C. Hao-Wen, H. Tianyi, L. Yuqiang, W. Chaochen, Z. Chenhui, Y. Wei, Z. Xiaowei and Y. Yang, *Advanced Materials*, 2018, 0, 1801501.
22. X. Xu, G. Zhang, L. Yu, R. Li and Q. Peng, *Advanced Materials*, 2019, 31, 1906045.
23. S. Li, L. Zhan, F. Liu, J. Ren, M. Shi, C.-Z. Li, T. P. Russell and H. Chen, *Advanced Materials*, 2017, 30, 1705208.
24. C. Li, Y. Xie, B. Fan, G. Han, Y. Yi and Y. Sun, *Journal of Materials Chemistry C*, 2018, 6, 4873-4877.
25. Z. Kang, S.-C. Chen, Y. Ma, J. Wang and Q. Zheng, *ACS Applied Materials & Interfaces*, 2017, 9, 24771-24777.
26. Z. Zhang, M. Li, Y. Liu, J. Zhang, S. Feng, X. Xu, J. Song and Z. Bo, *Journal of Materials Chemistry A*, 2017, 5, 7776-7783.
27. N. Qiu, H. Zhang, X. Wan, C. Li, X. Ke, H. Feng, B. Kan, H. Zhang, Q. Zhang, Y. Lu and Y. Chen, *Advanced Materials*, 2017, 29, 1604964.
28. Y.-T. Hsiao, C.-H. Li, S.-L. Chang, S. Heo, K. Tajima, Y.-J. Cheng and C.-S. Hsu, *ACS Applied Materials & Interfaces*, 2017, 9, 42035-42042.
29. Q. Cao, W. Xiong, H. Chen, G. Cai, G. Wang, L. Zheng and Y. Sun, *Journal of Materials Chemistry A*, 2017, 5, 7451-7461.
30. P. Yin, T. Zheng, Y. Wu, G. Liu, Z.-G. Zhang, C. Cui, Y. Li and P. Shen, *Journal of Materials Chemistry A*, 2018, 6, 20313-20326.
31. Q. Tu, Y. Ma, X. Zhou, W. Ma and Q. Zheng, *Chemistry of Materials*, 2019, 31, 5953-5963.
32. L. Feng, J. Yuan, Z. Zhang, H. Peng, Z.-G. Zhang, S. Xu, Y. Liu, Y. Li and Y. Zou, *ACS Applied Materials & Interfaces*, 2017, 9, 31985-31992.
33. J. Yuan, T. Huang, P. Cheng, Y. Zou, H. Zhang, J. L. Yang, S.-Y. Chang, Z. Zhang, W. Huang, R. Wang, D. Meng, F. Gao and Y. Yang, *Nature Communications*, 2019, 10, 570.
34. M. Luo, L. Zhou, J. Yuan, C. Zhu, F. Cai, J. Hai and Y. Zou, *Journal of Energy Chemistry*, 2020, 42, 169-173.
35. J. Yuan, Y. Zhang, L. Zhou, C. Zhang, T.-K. Lau, G. Zhang, X. Lu, H.-L. Yip, S. K. So, S. Beaupré, M. Mainville, P. A. Johnson, M. Leclerc, H. Chen, H. Peng, Y. Li and Y. Zou, *Advanced Materials*, 2019, 31, 1807577.
36. Z. Zhang, T. Shan, Y. Zhang, L. Zhu, L. Kong, F. Liu and H. Zhong, *Journal of Materials Chemistry C*, 2020, 8, 4357-4364.